Neapolitan Volcanoes


APAT
Agenzia per la Protezione dell'Ambiente e per i Servizi Tecnici
Dipartimento Difesa del Suolo
Servizio Geologico d'Italia
GEOLOGICAL MAP OF ITALY
1:1 250 000 Scale
MAIN TECTONO-STRATIGRAPHIC UNITS
SPECIALLY PRINTED FOR THE 32nd INTERNATIONAL GEOLOGICAL CONGRESS
ITALIA 2004

Three Volcanic Regions

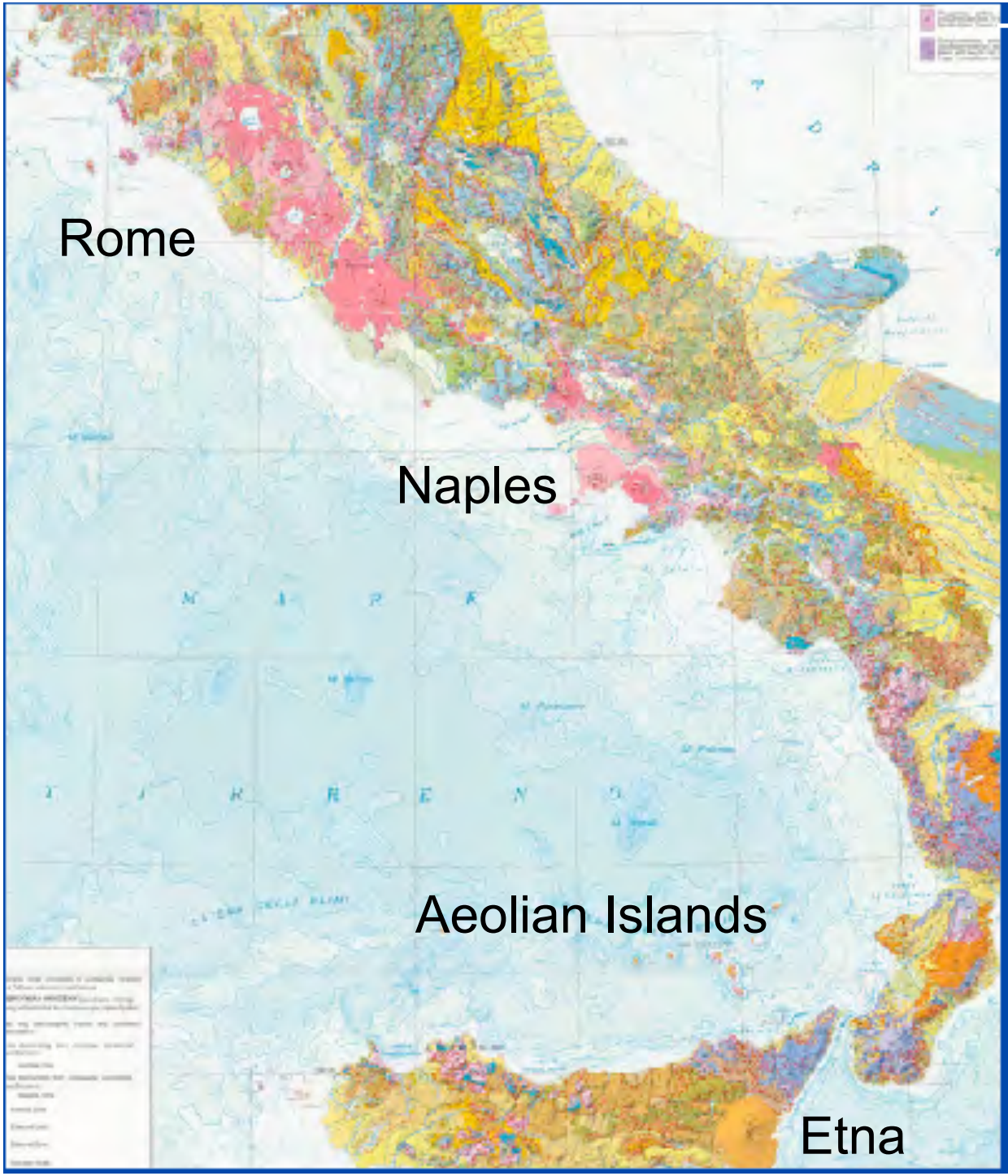

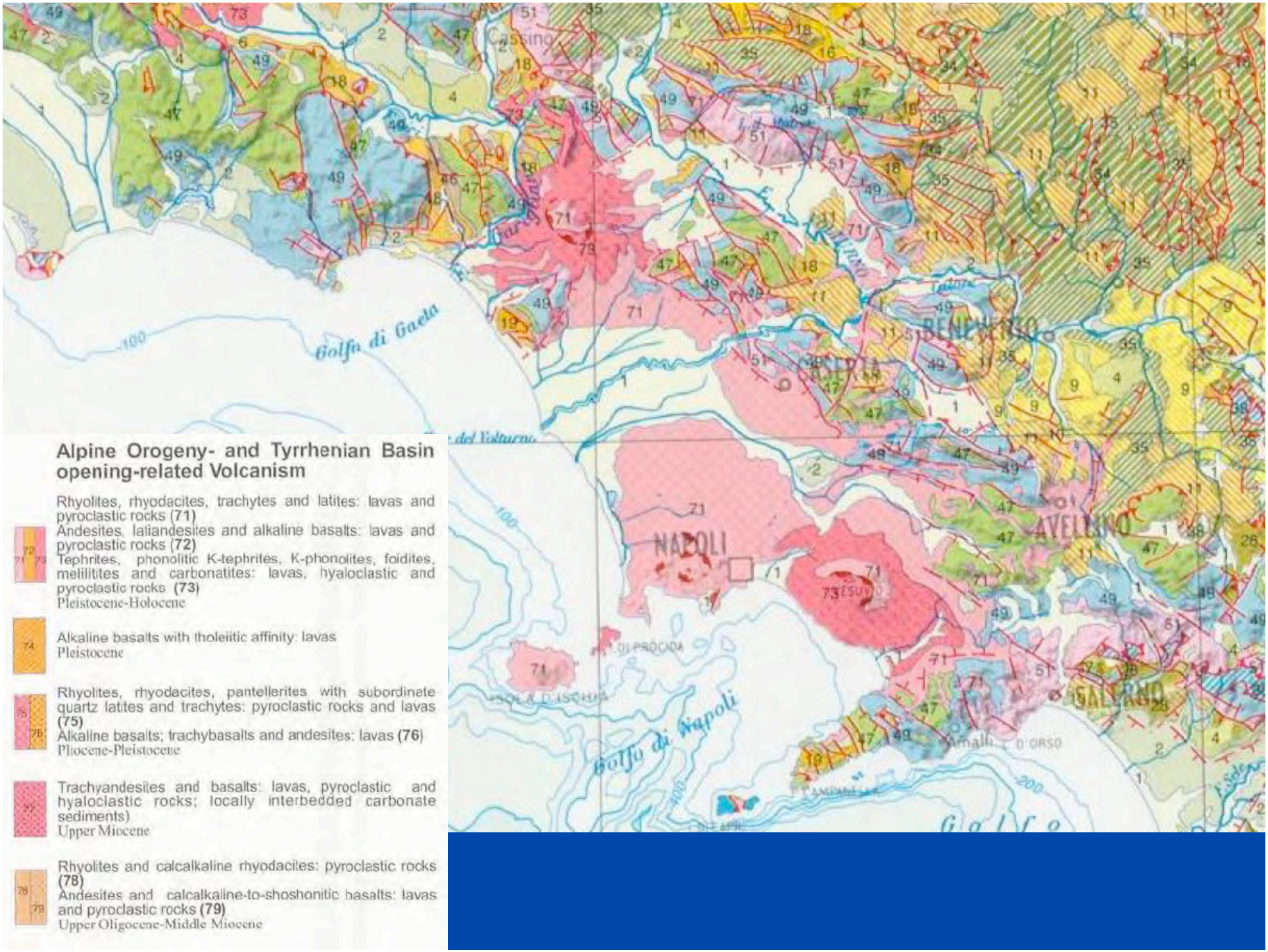

Alpine Orogeny- and Tyrrhenian Basin opening-related Volcanism

71 72 73 — Rhyolites, rhyodacites, trachytes and latites: lavas and pyroclastic rocks (**71**)
Andesites, latiandesites and alkaline basalts: lavas and pyroclastic rocks (**72**)
Tephrites, phonolitic K-tephrites, K-phonolites, foidites, melilitites and carbonatites: lavas, hyaloclastic and pyroclastic rocks (**73**)
Pleistocene-Holocene

74 — Alkaline basalts with tholeiitic affinity: lavas
Pleistocene

75 76 — Rhyolites, rhyodacites, pantellerites with subordinate quartz latites and trachytes: pyroclastic rocks and lavas (**75**)
Alkaline basalts; trachybasalts and andesites: lavas (**76**)
Pliocene-Pleistocene

77 — Trachyandesites and basalts: lavas, pyroclastic and hyaloclastic rocks; locally interbedded carbonate sediments)
Upper Miocene

78 79 — Rhyolites and calcalkaline rhyodacites: pyroclastic rocks (**78**)
Andesites and calcalkaline-to-shoshonitic basalts: lavas and pyroclastic rocks (**79**)
Upper Oligocene-Middle Miocene

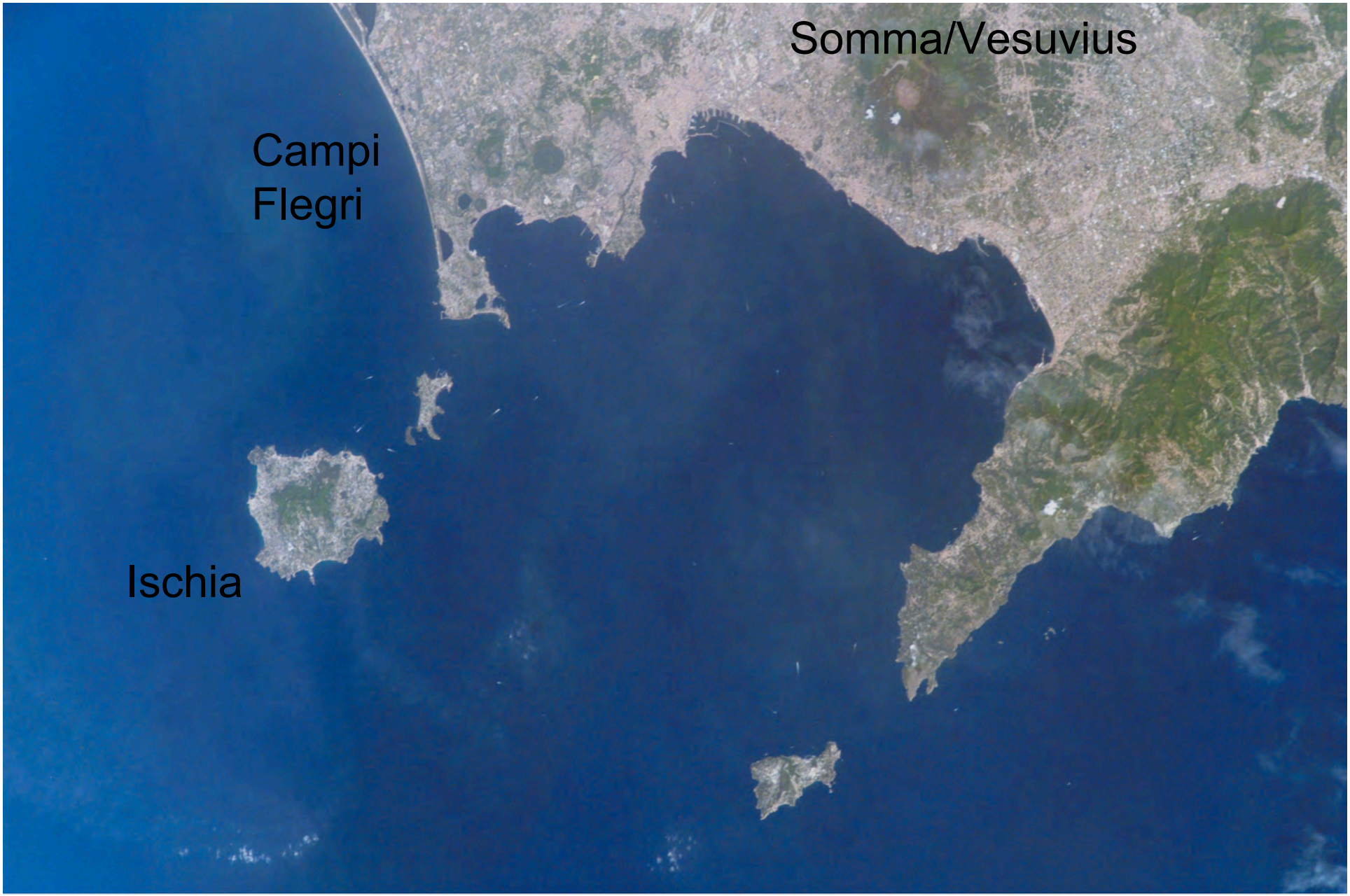

ISS015E09021

Bay of Naples

http://eol.jsc.nasa.gov/

ISS018E034177

Bay of Naples, Vesuvius, Phlegrian Fields

http://eol.jsc.nasa.gov/

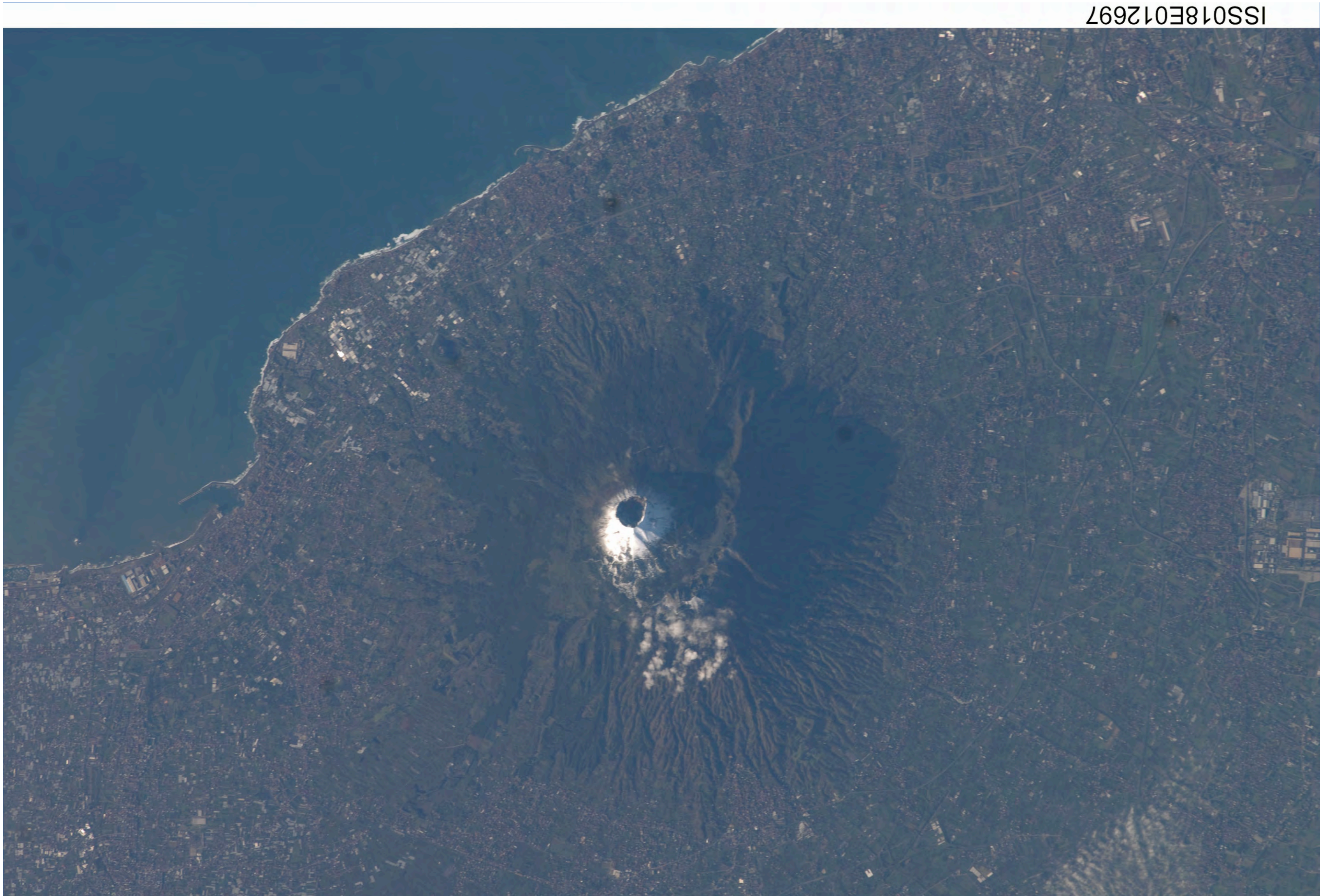

Vesuvius

http://eol.jsc.nasa.gov/

Monte Somma and Vesuvius from Naples

Monte Somma from Observatorio Vesuvio

Summit Crater Monte Somma

1943 Crater Vesuvius

1943 North Crater Wall, Vesuvius

Bay of Naples from Vesuvius rim, Herculeneum in middle distance

Herculeneum

Palestra, Herculeneum

Pyroclastic flow deposit, Herculeneum

Seaside arcades at Herculeneum nb central arcade

Pliny the Younger described the eruption cloud as a “pine tree”

What’s wrong with this image?

Campi Flegri

Lago Avenno, Campi Flegri

Solfaterra, Campi Flegri

Ischia, Bay of Naples

Ischia: lavas and dike, Bay of Naples

Somma and Vesuvius from Ischia, Bay of Naples

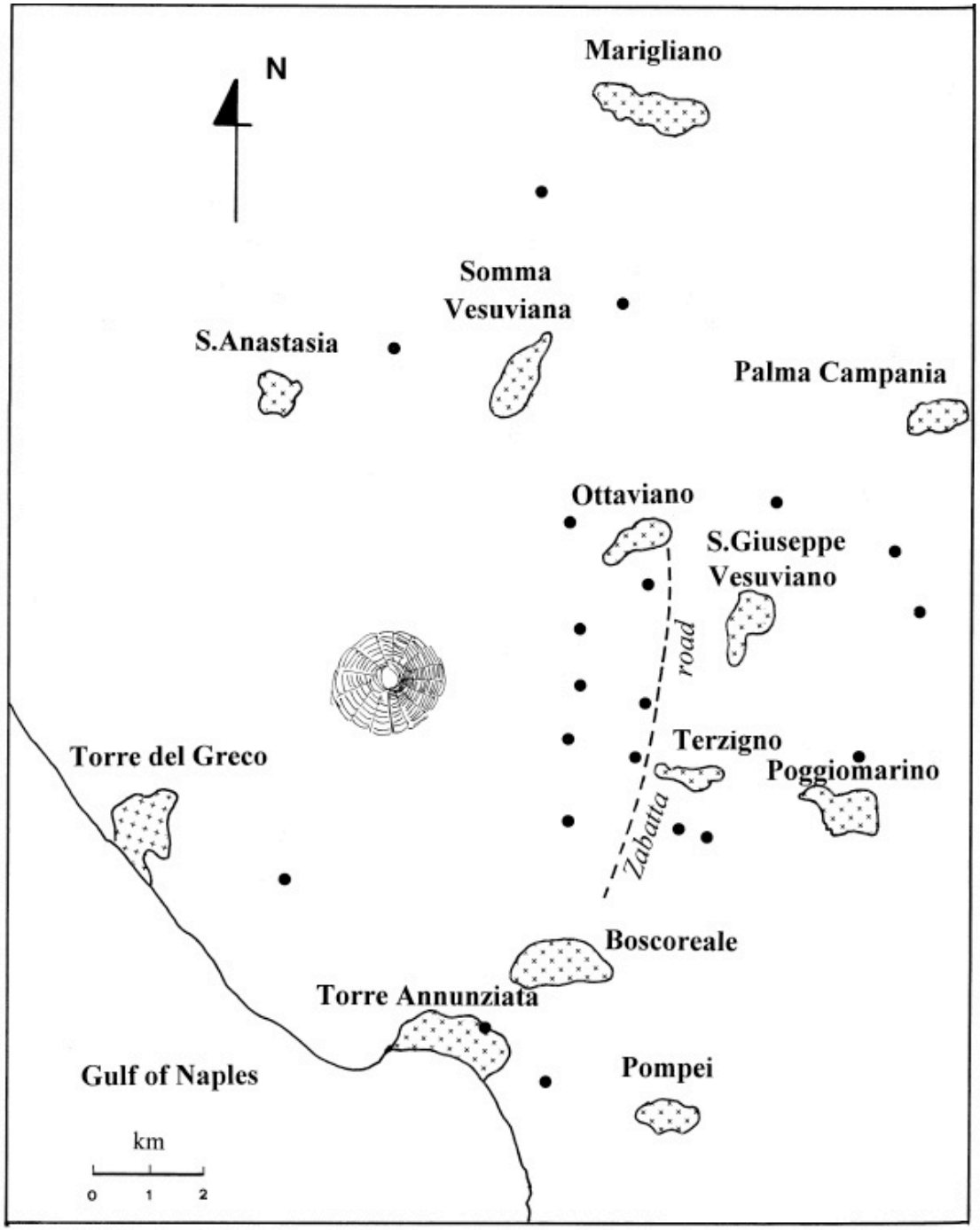

Fig. 1. Location map of investigated sites (●).

Rolandi et al 1998

Somma-Vesuvius

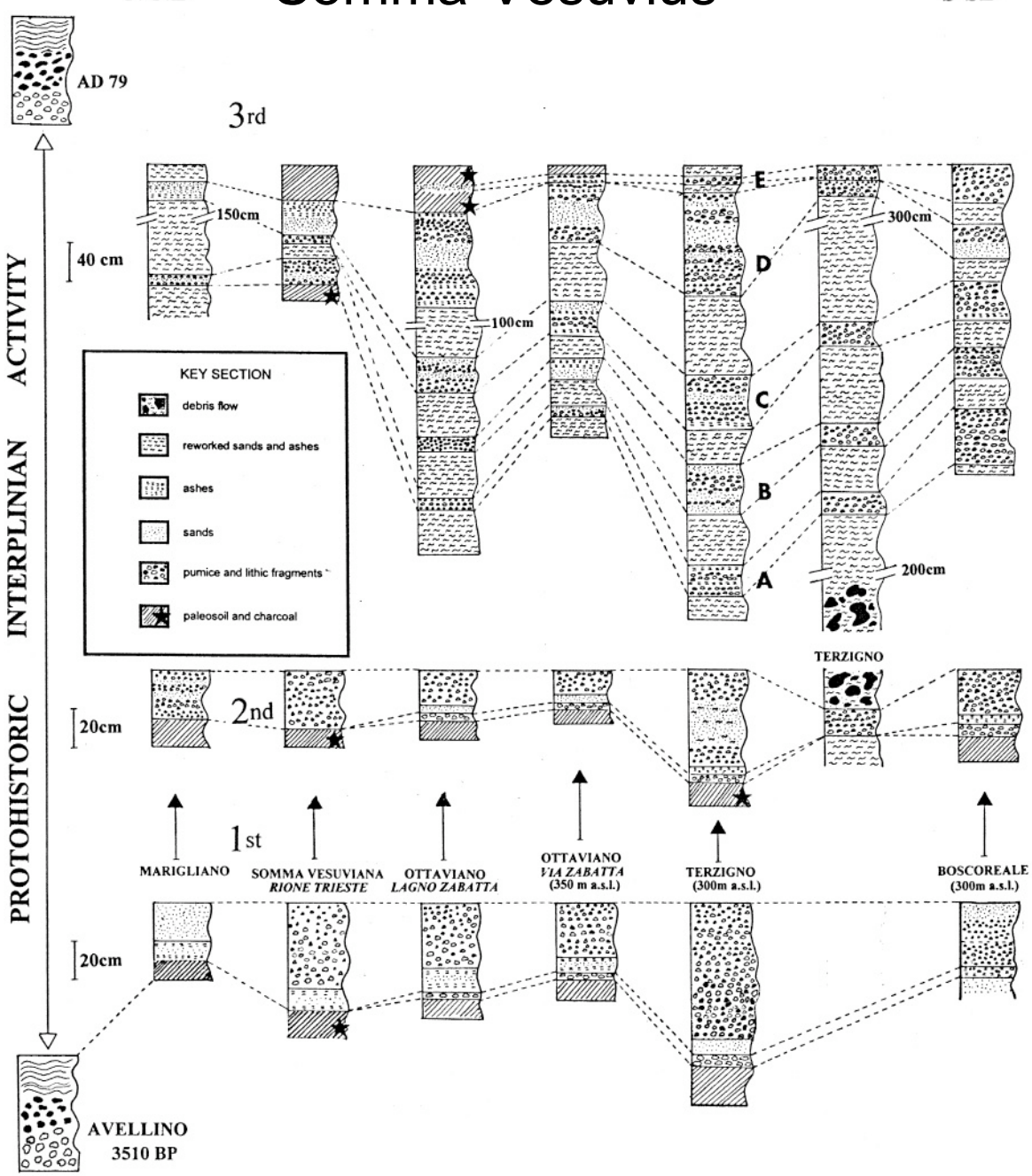

Fig. 2. Stratigraphic correlations in the proximal area among the investigated sections for protohistoric eruptions.

Rolandi et al 1998

Somma-Vesuvius

Table 1
Summarized features of layers forming the type sections of protohistoric tephra deposits

Unit	Maximum thickness (cm)	Locality	Sub-unit (from base to top)	Color	Grain size	Components	Grading	Md_Φ base	Md_Φ middle	Md_Φ top	σ_Φ base	σ_Φ middle	σ_Φ top
First protohistoric eruption													
a	11	Terzigno (300 m a.s.l.)	—	white	lapilli	pumice (vesiculated)	reverse to normal		−2.2			2.03	
b	10	Terzigno (300 m a.s.l.)	—	grey	ash	compacted pisolitic ash	ungraded		2.21			2.22	
c	60	Terzigno (300 m a.s.l.)	c_1 (42 cm)	dark	lapilli	dark unvesiculated pumice	normal	−0.39		0.78	1.347		1.731
			c_2 (18 cm)	dark	lapilli	in black sandy matrix	normal	0.278		0.50	1.371		1.817
Second protohistoric eruption													
a	6	Terzigno (300 m a.s.l.)	—	white	lapilli	pumice (vesiculated)	ungraded		−2.182			2.082	
b	4	Terzigno (300 m a.s.l.)	—	grey	ash	compacted ash	ungraded		1.952			1.861	
c	45	Terzigno (300 m a.s.l.)	—	dark grey	lapilli	dark pumice in black sandy matrix	normal to reverse	−1.15	−0.037	−1.556	1.578	1.8	1.534
d	41	Terzigno (300 m a.s.l.)	—	dark grey	lapilli	compacted sand	ungraded		1.091			2.224	
Third protohistoric eruption													
A	32	Boscoreale (300 m a.s.l.)	A_1 (6 cm)	black	lapilli	pumice in sandy matrix	normal		0.511			1.095	
			A_2 (3 cm)	black	lapilli	sand	ungraded		—			—	
			A_3 (23 cm)	black	lapilli	pumice in sandy matrix	normal to reverse		0.109			1.635	
B	47	Terzigno (300 m a.s.l.)	B_1 (46 cm)	black	lapilli	medium to coarse sand	reverse to normal	0.28	−1.042		1.407	1.946	1.697
			B_2 (1 cm)	white	lapilli	pumice	ungraded		−0.313				2.576
C	70	Ottaviano Lagno Zabatta (300 m a.s.l.)	C_1 (15 cm)	black	ash	compacted ash	ungraded		3.25				1.759
			C_2 (29 cm)	black	lapilli	pumice in sandy matrix	reverse to normal		−0.4				1.527
			C_3 (2 cm)	black	lapilli	compacted sand	ungraded		1.9				2.019
			C_4 (12 cm)	black-red	lapilli	sand	reverse graded	−1.297			0.767	1.218	
			C_5 (12 cm)	black	lapilli	sand	laminated	2.267	0.107		4.07	2.168	1.626
D	113	Ottaviano Lagno Zabatta (300 m a.s.l.)	D_1 (51 cm)	black	lapilli-ash	pumice-ash	laminated		−0.219				1.207
			D_2 (3 cm)	black	lapilli	fine sand	ungraded		0.571				1.442
			D_3 (23 cm)	black-red	lapilli	scoria-lithic fragments	reverse to normal	−0.615			−1.515	1.73	
			D_4 (3 cm)	ochre	lapilli	pumice	ungraded		0.65				2.654
			D_5 (11 cm)	black-red	lapilli	sand	ungraded		0.57				1.44
			D_6 (10 cm)	white	lapilli	vesiculated pumice	normal		−3.18				1.57
			D_7 (10 cm)	leaden	lapilli	scoria-lithic fragments	ungraded		−0.857				1.37
			D_8 (2 cm)	leaden	ash	compacted ash	ungraded		—				—
E	45	Ottaviano Lagno Zabatta (300 m a.s.l.)	E_1 (7 cm)	black	ash	compacted ash	laminated		—				—
			E_2 (9 cm)	black	lapilli	fine sand	ungraded		—				—
			E_3 (29 cm)	black	lapilli	scoria-lithics	reverse graded		0.296				1.524

Rolandi et al 1998

Somma-Vesuvius

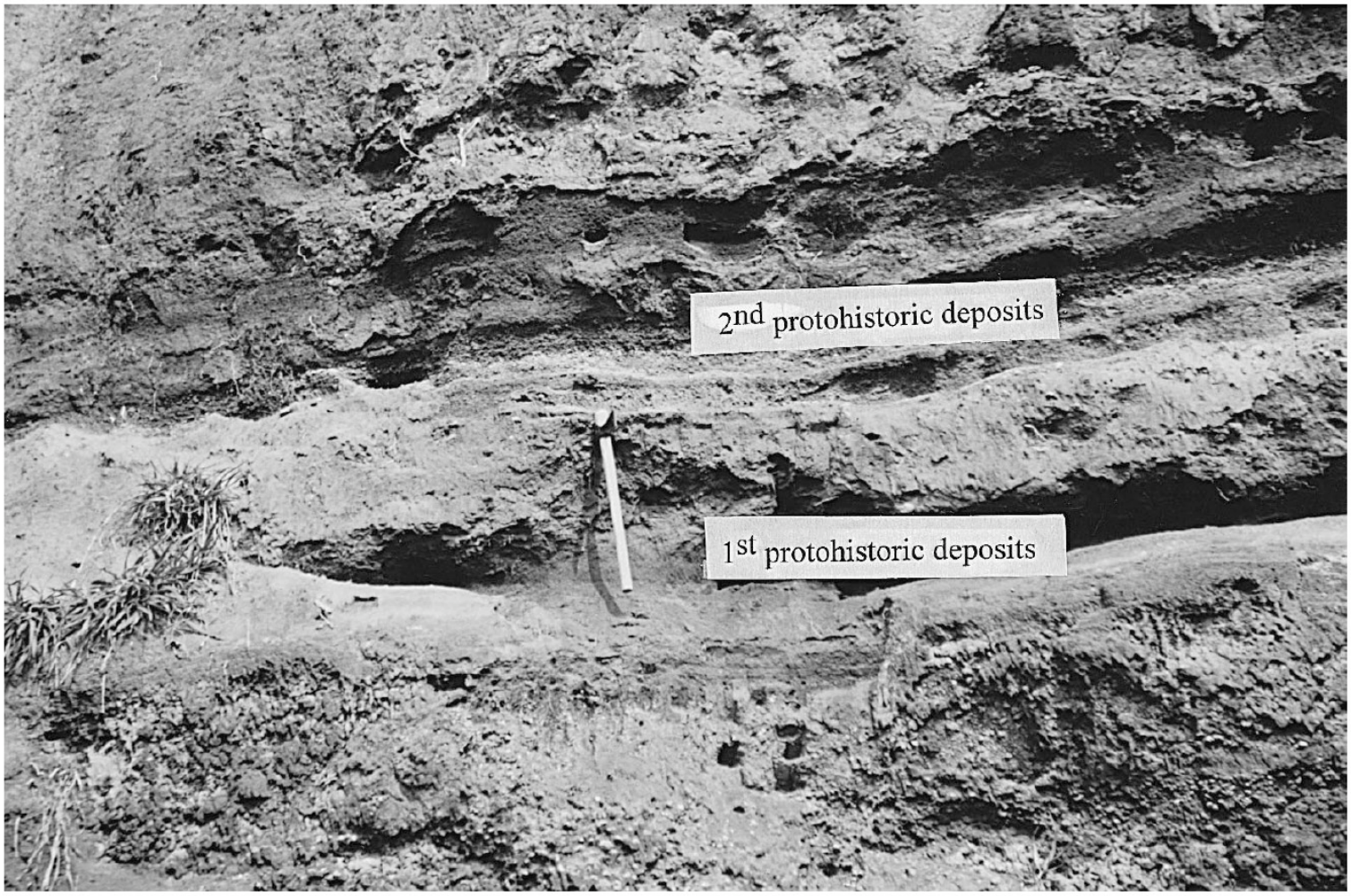

lucts of the first and second protohistoric eruption products at Marigliano (northeast of the vent). Note in this site the absence of umice layers (a), spread towards the southeast.

Rolandi et al 1998

Somma-Vesuvius

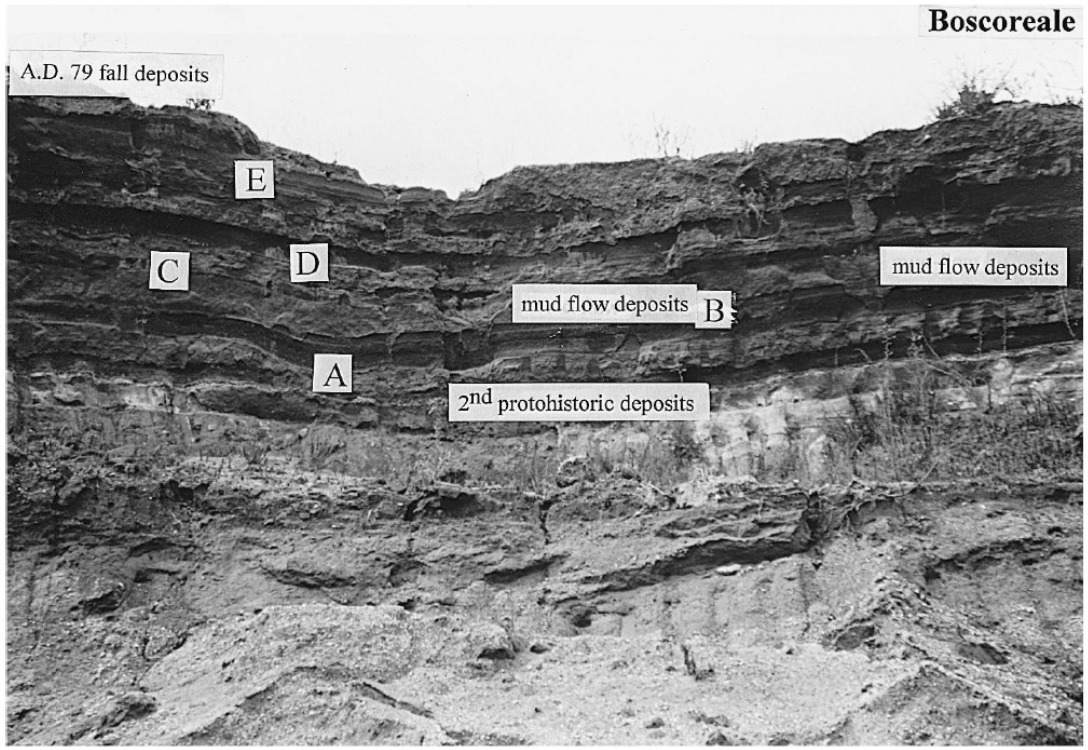

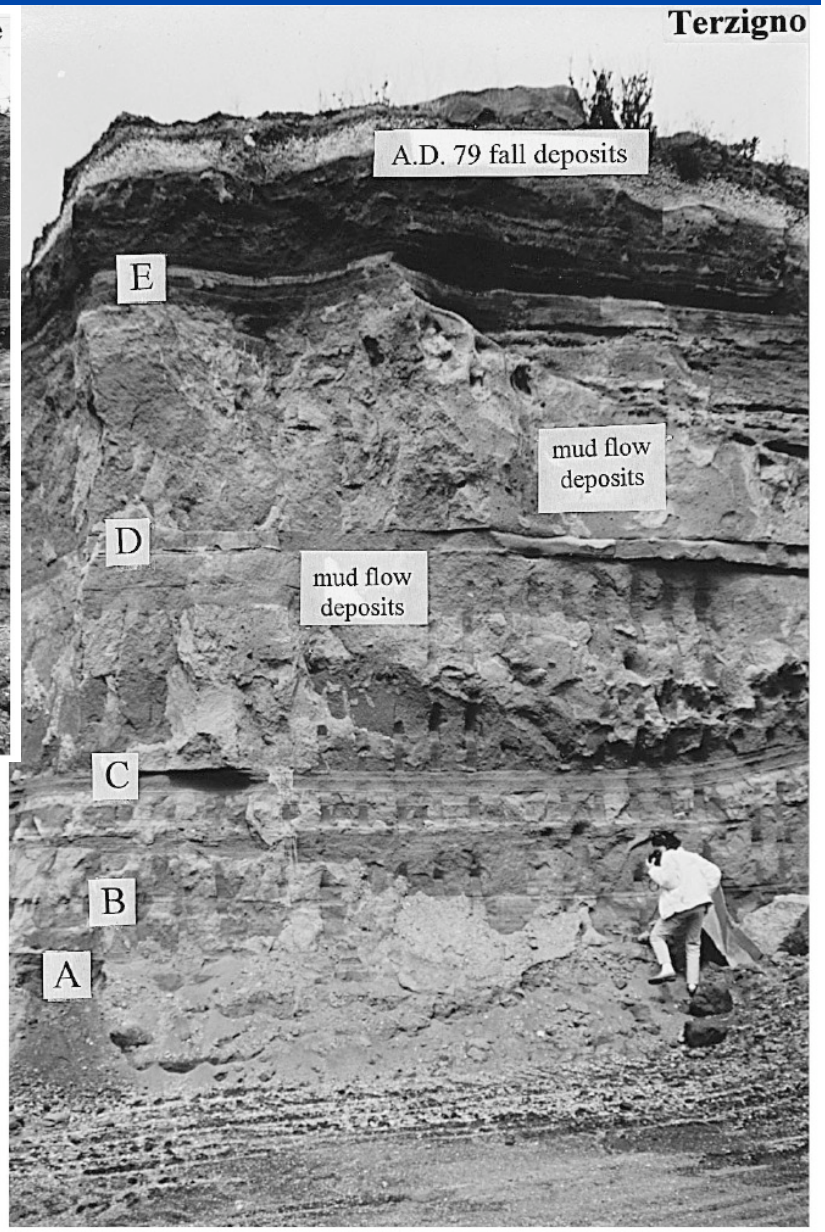

Rolandi et al 1998

Fig. 8. Products of the third protohistoric eruption at Boscoreale (300 m a.s.l.) and at Terzigno (50 m a.s.l.). Note that thicknesses of mud-flow deposits increase in the plain.

Somma-Vesuvius

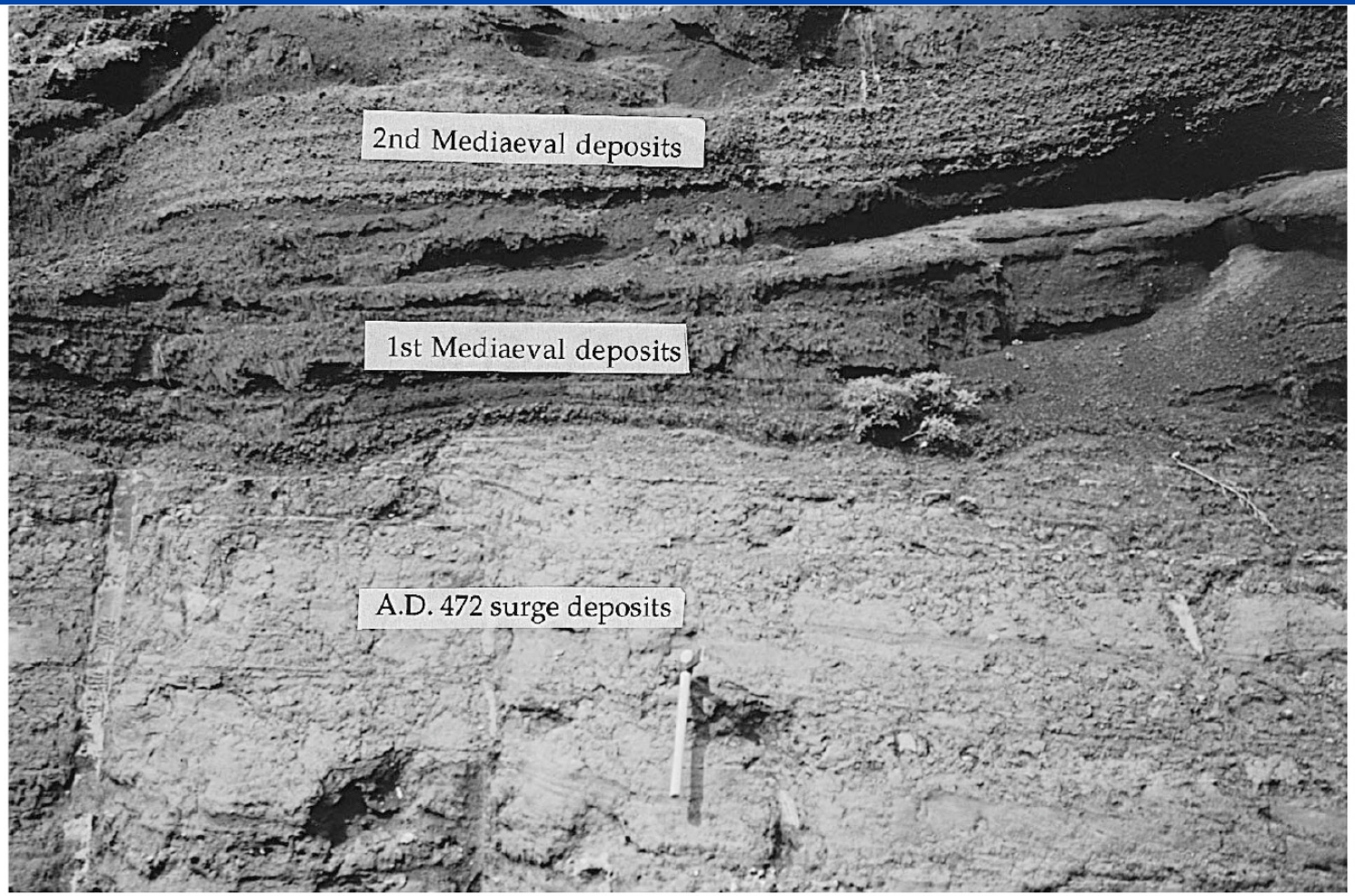

. Products of first and second medieval eruptions at Terzigno (300 m a.s.l.). Note the U-shaped erosional surface of A.D. 472 surge

Rolandi et al 1998

Somma-Vesuvius

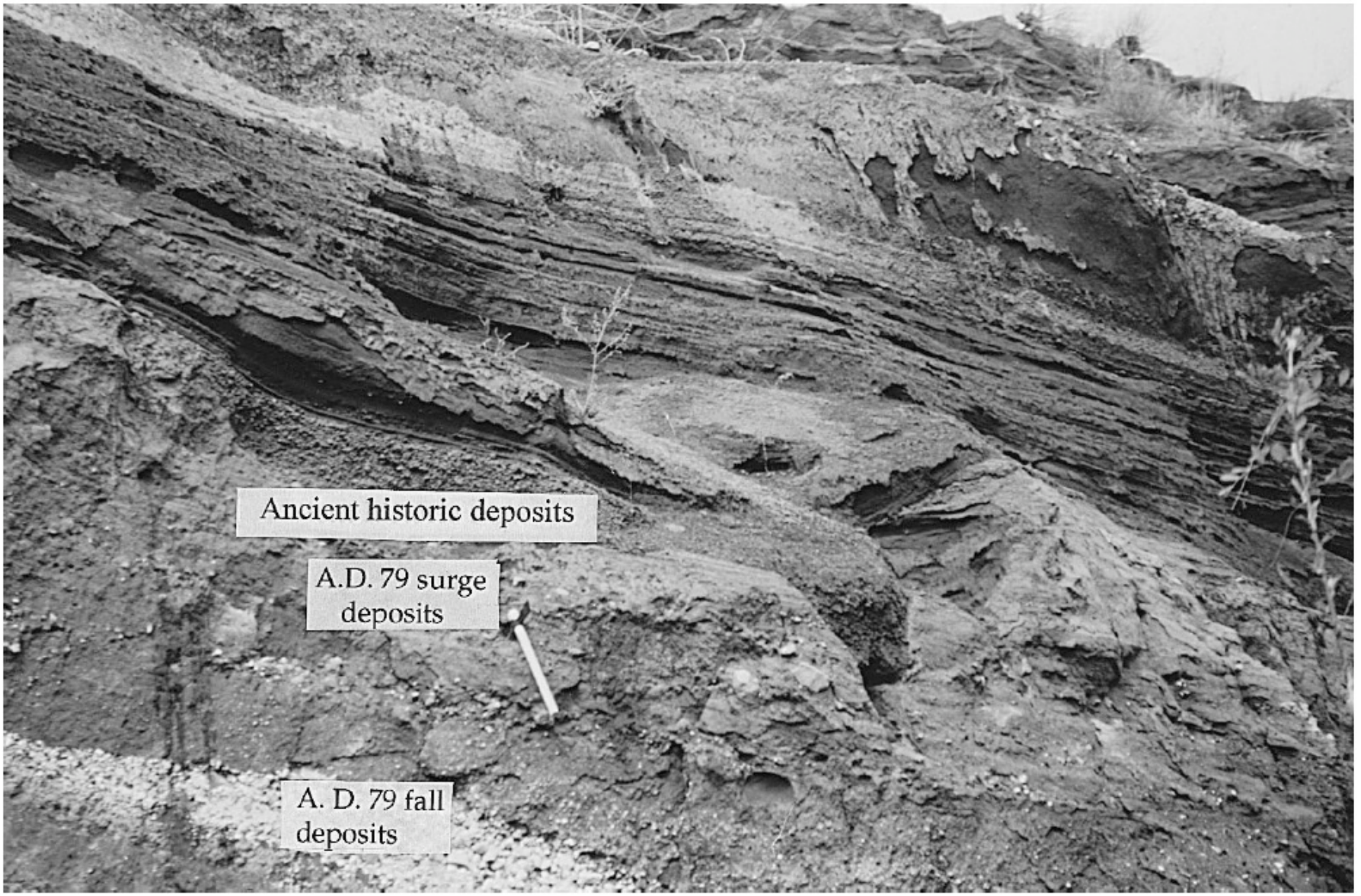

Fig. 9. Products of the ancient historic eruption at Terzigno (300 m a.s.l.).

Rolandi et al 1998

Somma-Vesuvius

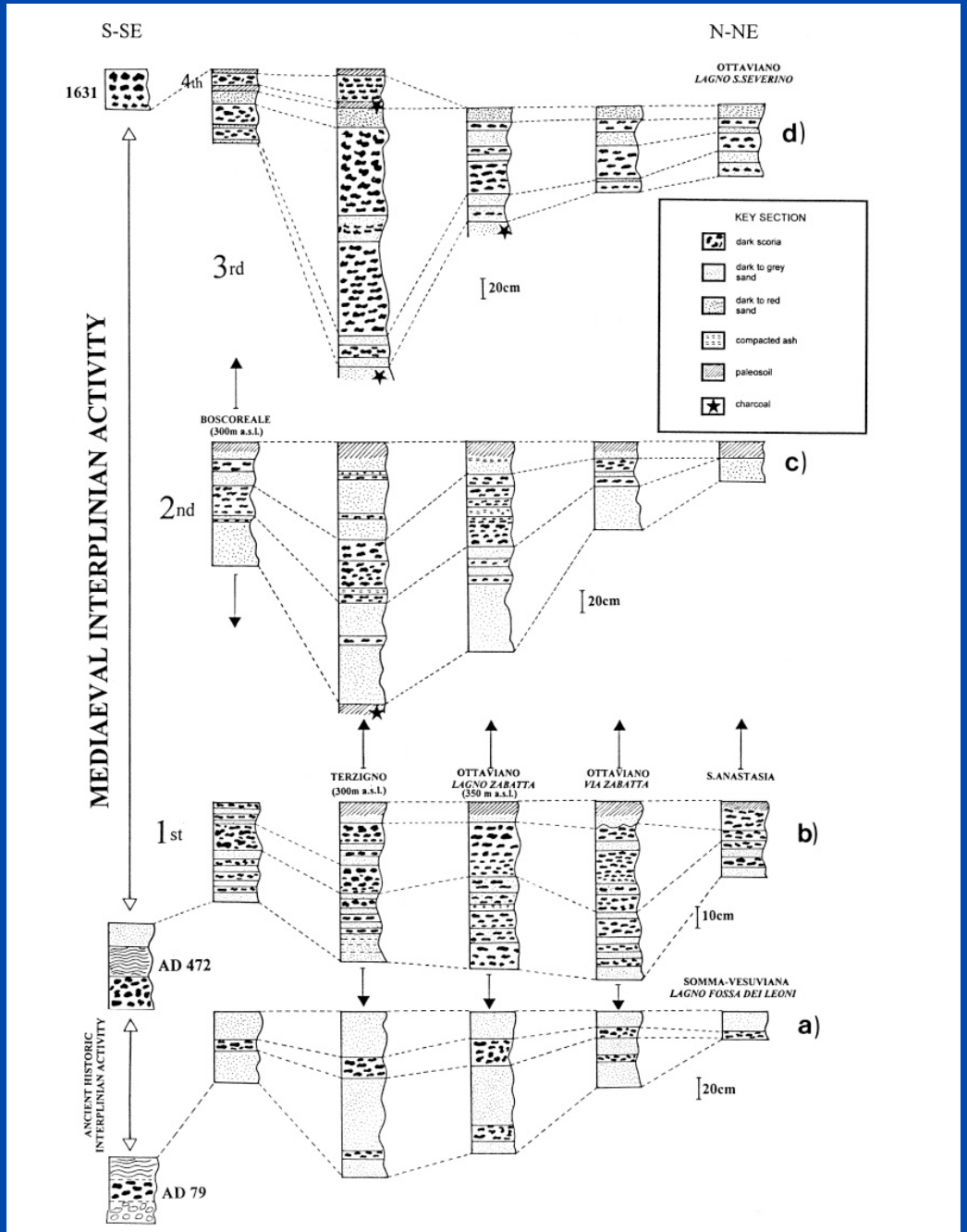

10. Stratigraphic correlations in the proximal area among the investigated sections for ancient historic (a) and medieval eruptions (b–d).

Rolandi et al 1998

Somma-Vesuvius

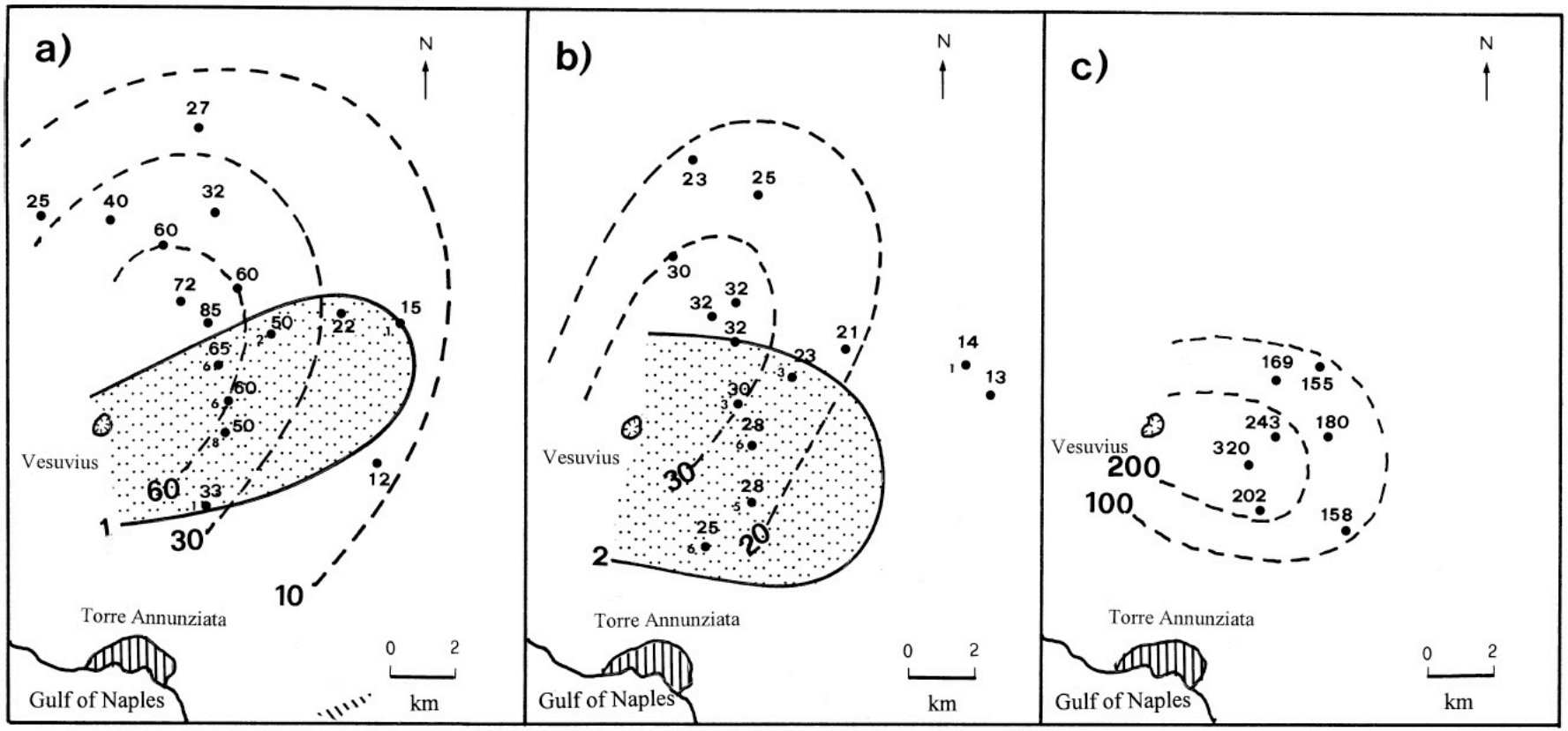

Fig. 5. (a) Isopach map of the first protohistoric eruption products. Dotted area and smaller numbers refer to layer a. (b) Isopach map of the second protohistoric eruption products. Dotted area and smaller numbers refer to layer a. (c) Isopach map of the third protohistoric eruption products. Thicknesses in cm.

Rolandi et al 1998

Somma-Vesuvius

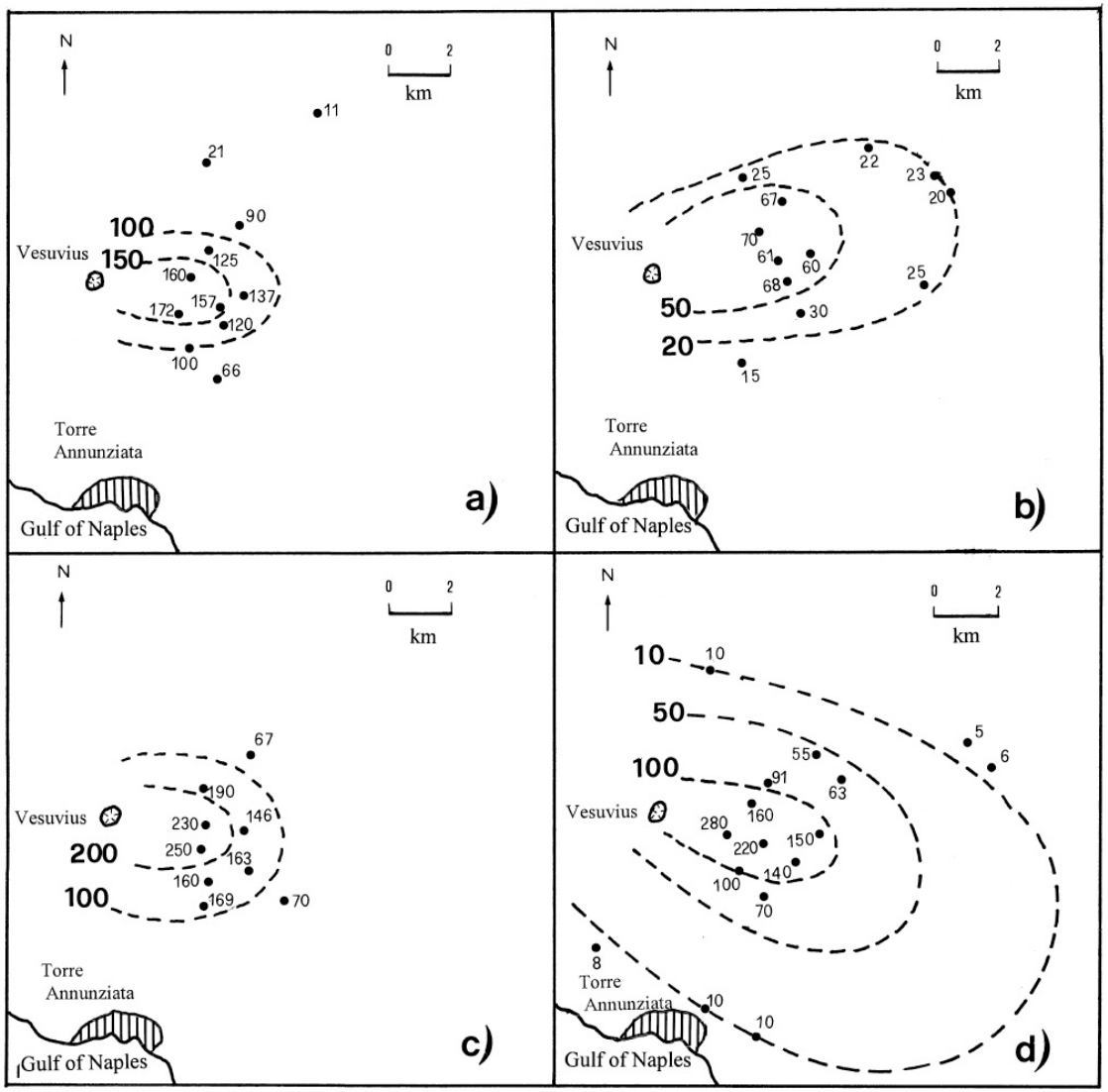

Fig. 12. (a) Isopach map of the ancient historic eruption products. (b) Isopach map of the first medieval eruption products. (c) Isopach map of the second medieval eruption products. (d) Isopach map of the third medieval eruption products. Thicknesses in cm.

Rolandi et al 1998

Somma-Vesuvius

^{14}C dating of investigated products

Eruption	Locality	Age (yr B.P.)	Calibrated age[a]	Material	Source	Sample
Prehistoric – protohistoric eruptions						
Avellino	Ottaviano	3548 ± 129	B.C. 2272 (1884) 1524	charcoal	Teledyne	
Avellino	Ottaviano	3240 ± 10	B.C. 1740 (1513)1276	organic material[b]	Teledyne	
First protohistoric	Somma–Vesuviana	3500 ± 60	B.C. 1967 (1868, 1843, 1776) 1676	charcoal[c]	USGS	WW-255
First protohistoric	Somma–Vesuviana	3480 ± 60	B.C. 1938 (1758) 1631	charcoal[c]	USGS	WW-517
First protohistoric	Somma–Vesuviana	3279 ± 60	B.C. 1938 (1758) 1631	charcoal[c]	Teledyne	
Second protohistoric	Somma–Vesuviana	3150 ± 100	B.C. 1626 (1414) 1129	charcoal[c]	USGS	W-6329
Second protohistoric	Somma–Vesuviana	3250 ± 70	B.C. 1681 (1516) 1395	charcoal[c]	USGS	WW-256
Second protohistoric	Somma–Vesuviana	3280 ± 70	B.C. 1734 (1522) 1409	charcoal[c]	USGS	WW-257
Third protohistoric phase A	Somma–Vesuviana	2710 ± 60	B.C. 989 (832) 794	charcoal[c]	USGS	WW-519
Third protohistoric phase B	Terzigno	3280 ± 70	B.C. 1620 (1522) 1461	charcoal[d]	USGS	WW-518
Third protohistoric phase C	Terzigno	3470 ± 70	B.C. 1945 (1748) 1611	charcoal[d]	USGS	WW-516
Third protohistoric phase E	Ottaviano	3120 ± 60	B.C. 1518 (1404) 1170	charcoal[d]	USGS	WW-259
A.D. 79	Ottaviano	2120 ± 60	B.C. 361 (157, 137, 125) A.D. 13	charcoal[c]	USGS	WW-260
Medieval eruptions						
A.D. 472	Terzigno	1590 ± 190	A.D. 59 (445) 861	charcoal[e]	Teledyne	
Second eruption	Ottaviano	1290 ± 40	A.D. 661 (771, 746, 755) 863	charcoal[c]	USGS	WW-6327
Second eruption	Terzigno	1440 ± 60	A.D. 537 (635) 692	charcoal[c]	USGS	WW-595
Third eruption	Terzigno	1140 ± 60	A.D. 775 (893) 1017	charcoal[e]	USGS	WW-596
Fourth eruption	Terzigno	950 ± 50	A.D. 1003 (1041, 1150) 1279	charcoal[c]	USGS	WW-597
Fourth eruption	Boscoreale	950 ± 90	A.D.895 (1041, 1150) 1279	charcoal[e]	Teledyne	

[a]Numbers in parentheses represent calendar years where ^{14}C age B.P. intercept calibrated tree ring curve. Numbers to left and right of parentheses represent 2 sigma range of calibrated calendar years (Stuiver and Pearson, 1993; Stuiver and Reimer, 1993).
[b]In prehistoric vase interbedded in the Avellino pumice-fall deposit.
[c]Charcoal interbedded in the products of the eruptions or in the underlying paleosoil.
[d]Charcoal interbedded in reworked material underlying the products of the eruption.

G. Rolandi et al. / Journal of Volcanology and Geothermal Research 82 (1998) 19–52

Rolandi et al 1998

Ischia

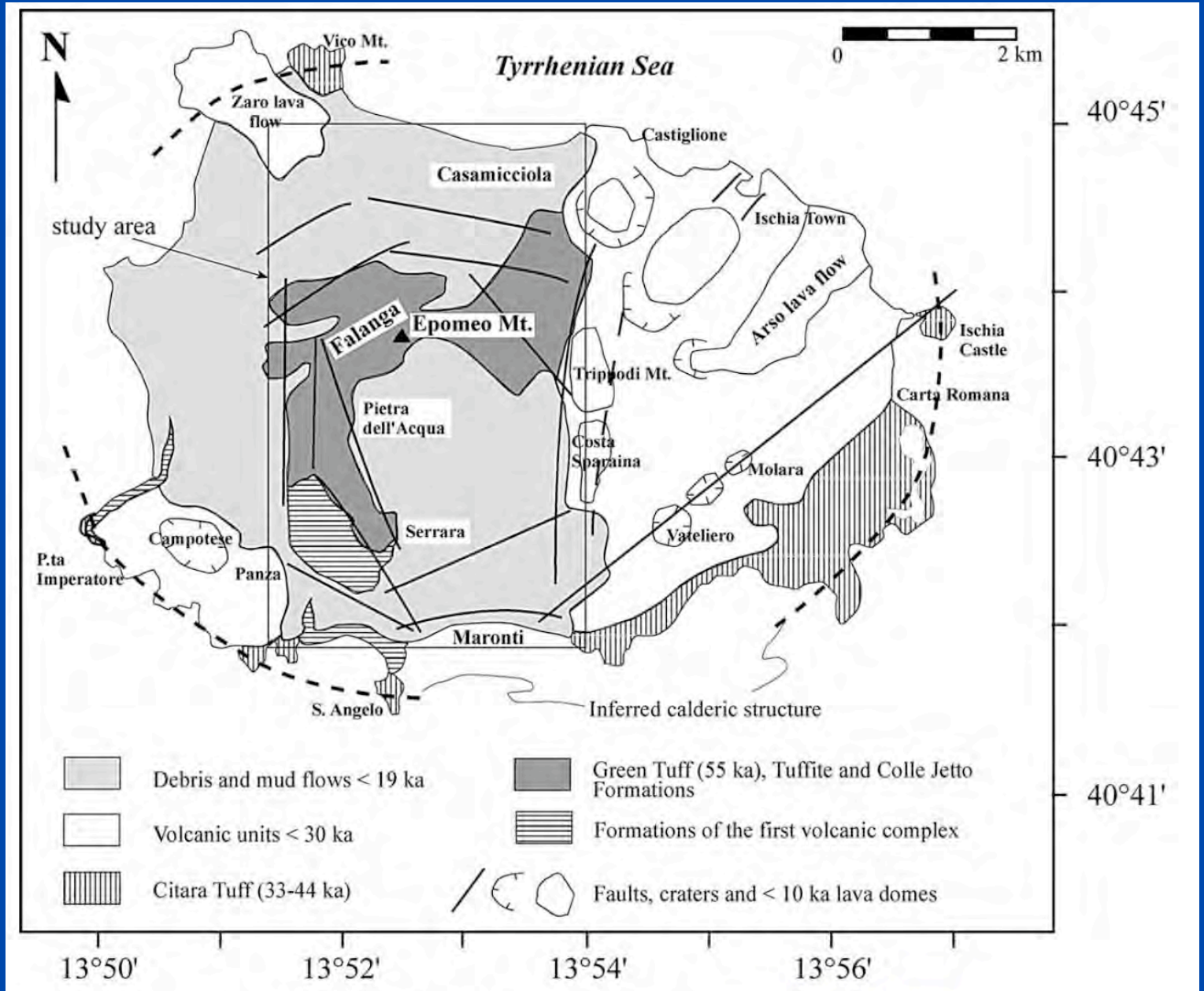

Fig. 2. Geological Map of Ischia Island, modified after Gillot et al. (1982).

Ischia

P. Molin et al. / Journal of Volcanology and Geothermal Research 121 (2003) 65–81

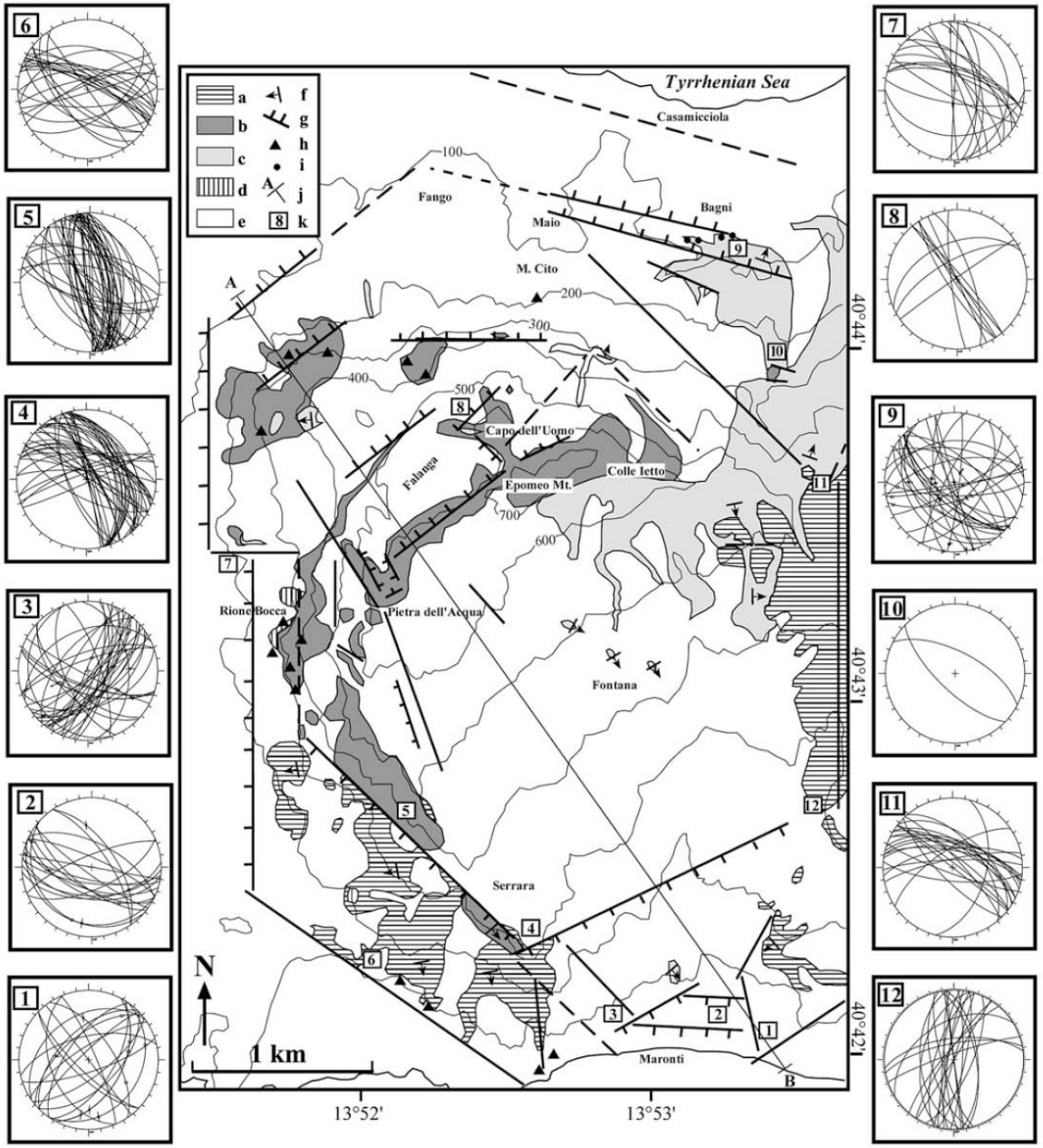

Ischia

P. Molin et al. / Journal of Volcanology and Geothermal Research 121 (2003) 65–81

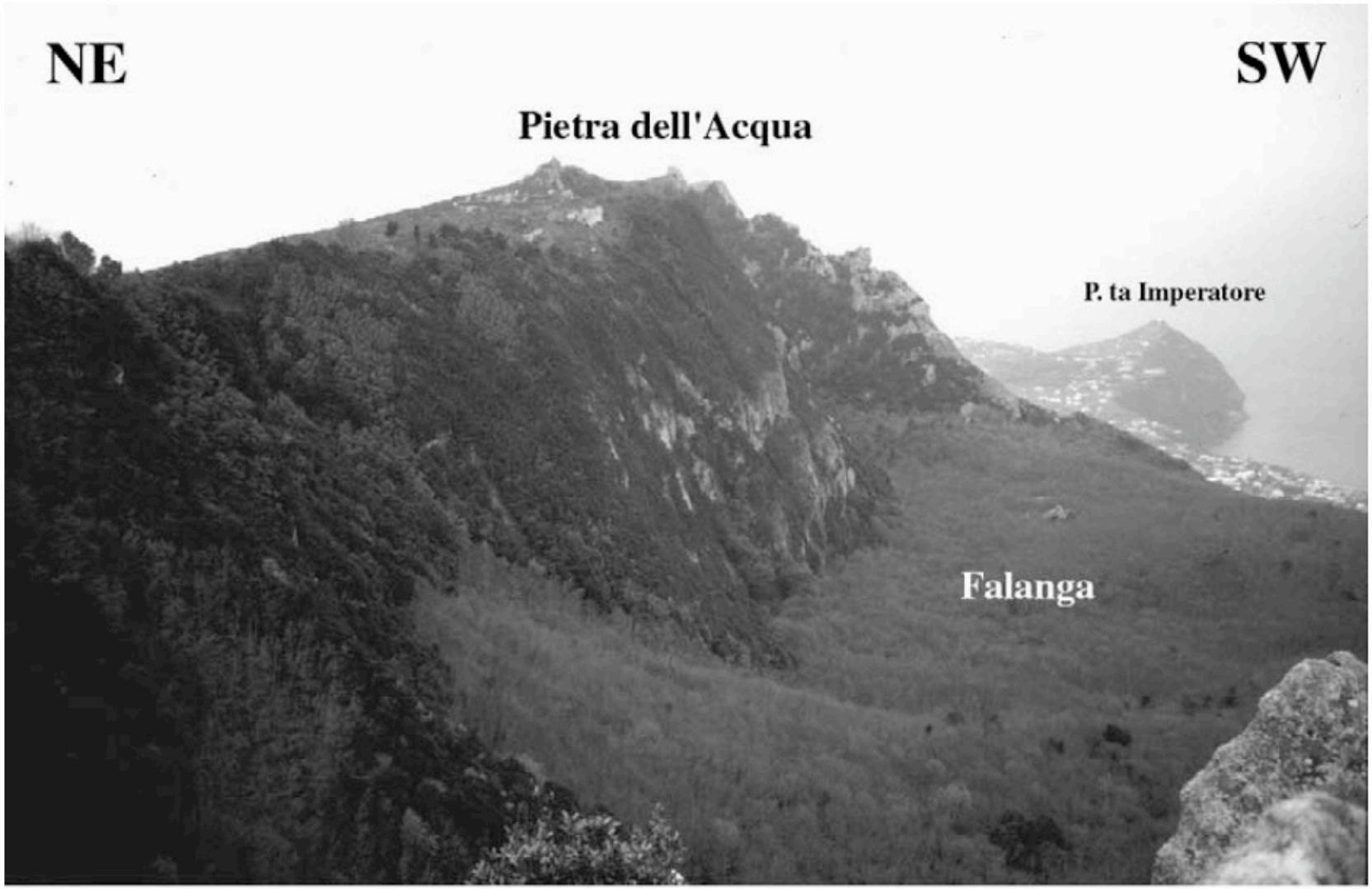

Fig. 4. View of the NE–SW-trending 200-m-high scarp at Falanga; the picture is taken from the NE.

Ischia

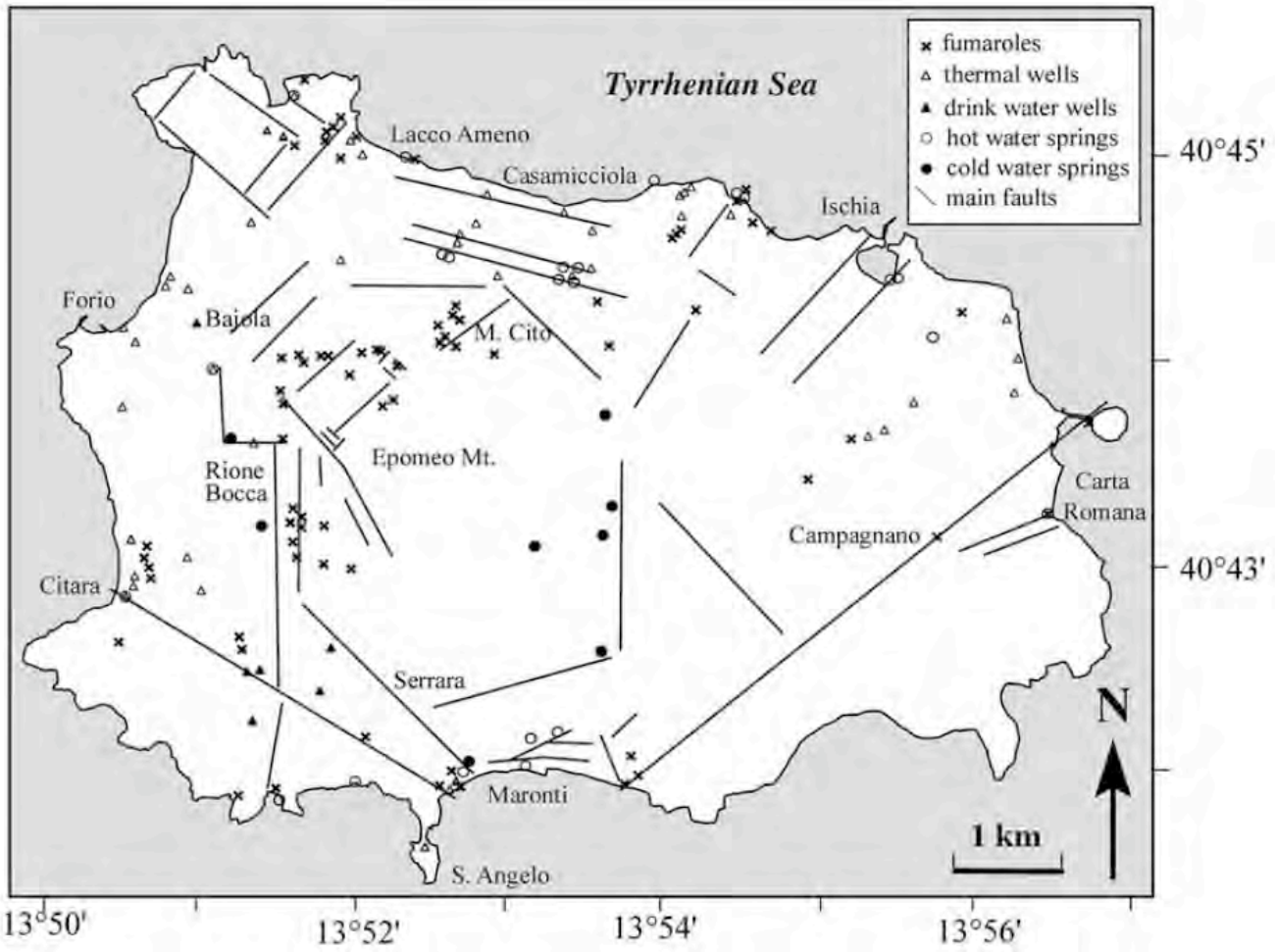

Fig. 6. Location of the fumarole fields, the cold and hot springs, the thermal and potable water wells, and the main tectonic structures at Ischia. These data are taken from the field survey, historical sources and, subordinately, from Santi (1955) and Vezzoli (1988).

Ischia

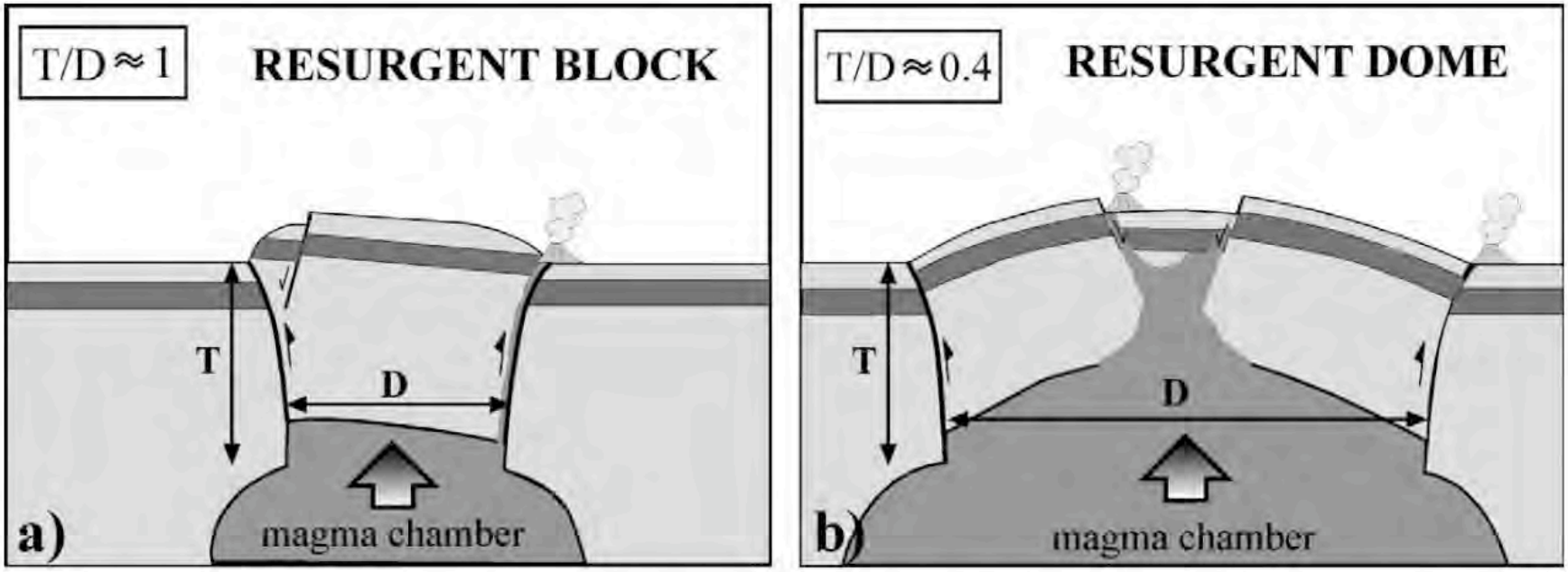

Fig. 1. Resurgence modalities observed in experiments and in nature as a function of the aspect ratio *A* (T/D) of the crust overlying the magma chamber. (a) A crust with higher *A* develops a resurgent block with uniformly-dipping layers within, and volcanic activity along the borders (Ischia and Pantelleria type). (b) A crust with lower *A* develops a resurgent dome with domed layers, a crestal depression and volcanic activity at the borders and within the dome (Valles and Long Valley type). (Modified after Acocella et al., 2001).

Ischia

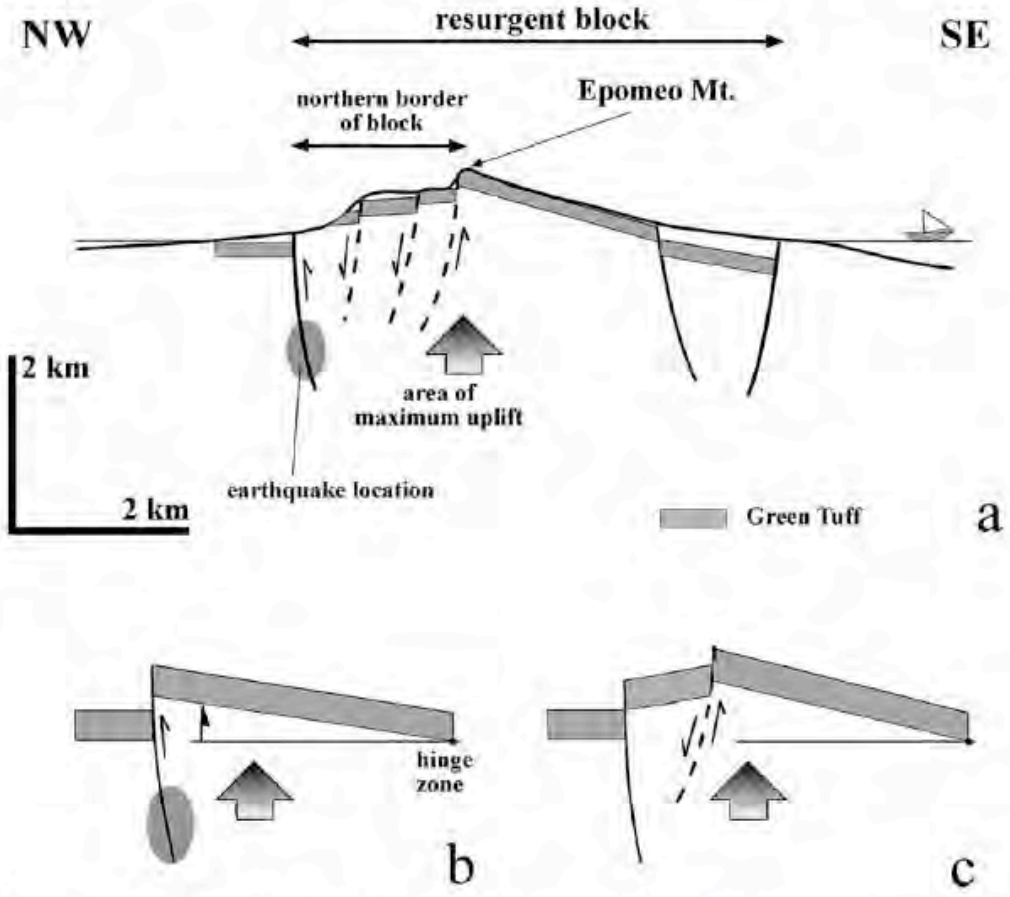

Fig. 8. Model for the rise of the resurgent block at Ischia. (a) Present situation. The asymmetric block is bordered by high-angle inward-dipping reverse faults. Outward-dipping normal faults are present in the innermost part, along the periphery of the block. As suggested by the interpretation of the macroseismic field (Cubellis, 1985; Cubellis and Luongo, 1998), seismic activity (shaded area) is located on the northern side of the block, in correspondence with the reverse faults, at a depth of 1–1.6 km. (b) Evolutionary model of the intermittent trapdoor uplift: seismic activity is triggered by the reverse faults on the most strained side of the block. (c) Evolutionary model of the intermittent trapdoor uplift: the activity of the reverse fault induces the collapse of the periphery of the block, forming the outward-dipping normal faults. The further reactivation of the outermost reverse faults triggers a new cycle of trapdoor uplift of the block. The combined activity of the reverse and normal faults along the periphery of the block is able to accommodate the space created by the resurgence.

Campo Flegrei

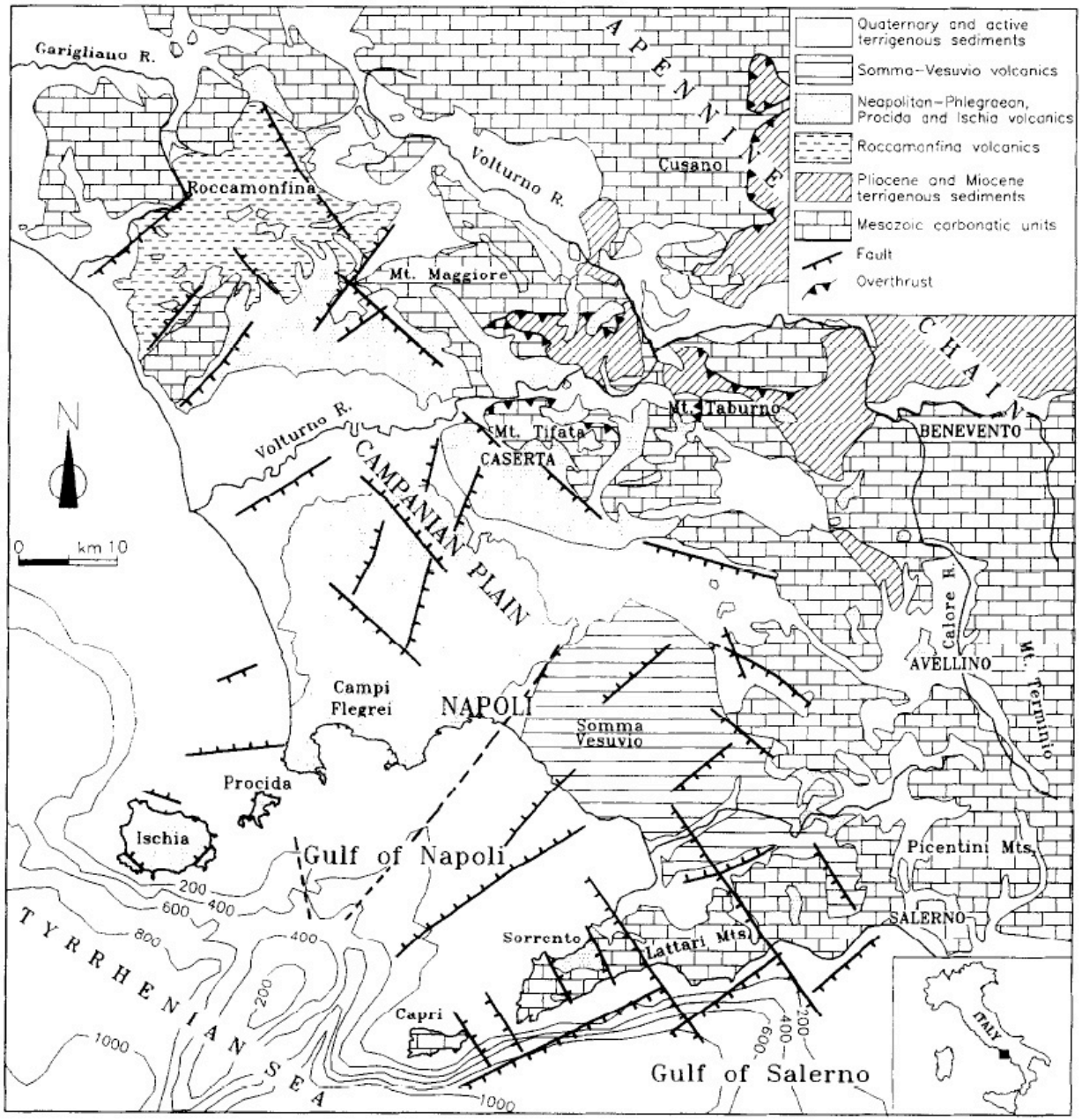

Fig. 1. Geological sketch map of the Campanian Plain and surroundings.

Orsi et al 1996

Campo Flegrei

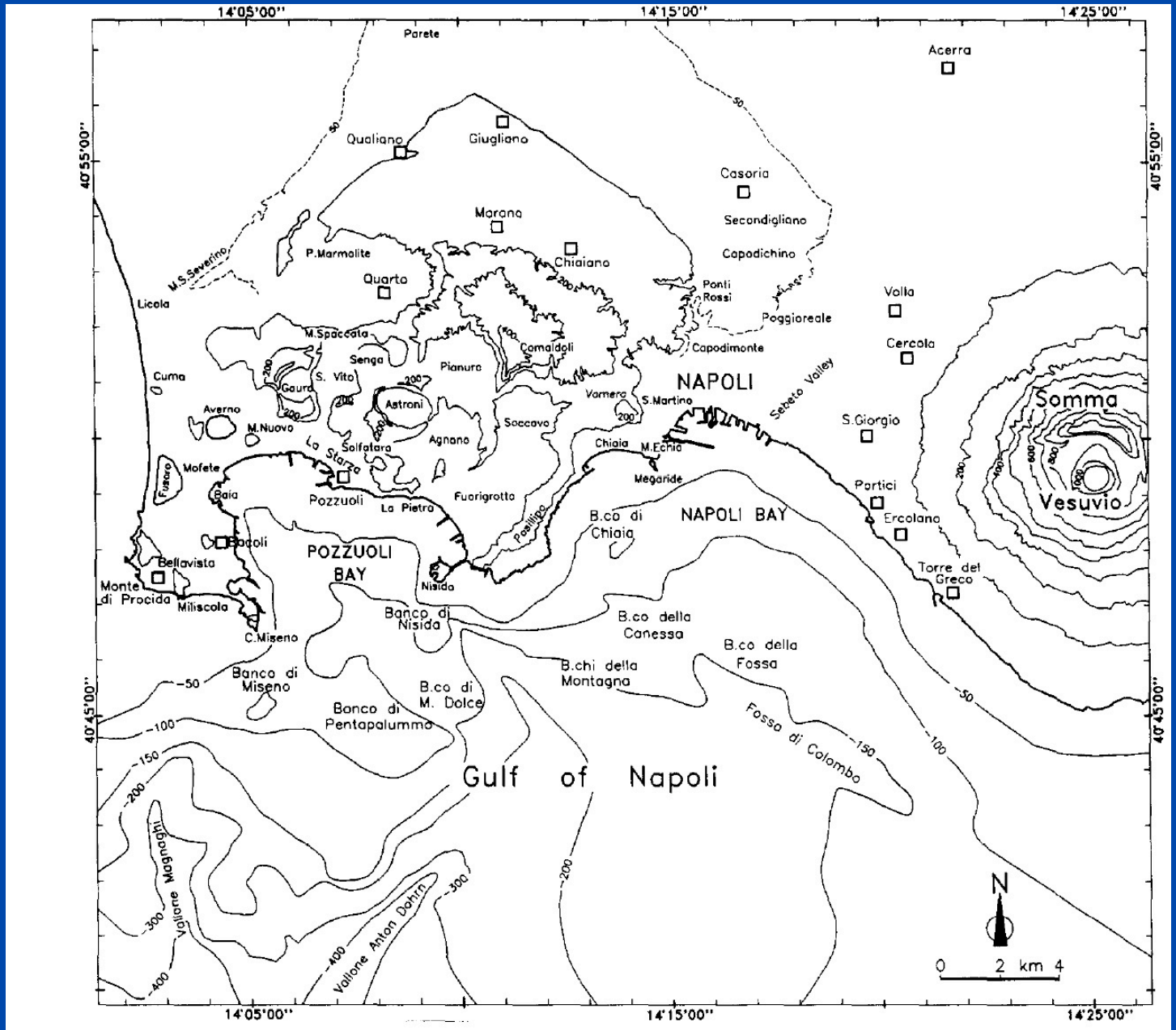

Fig. 2. Morphological map of the Neapolitan–Phlegrean area.

Orsi et al 1996

Campo Flegrei

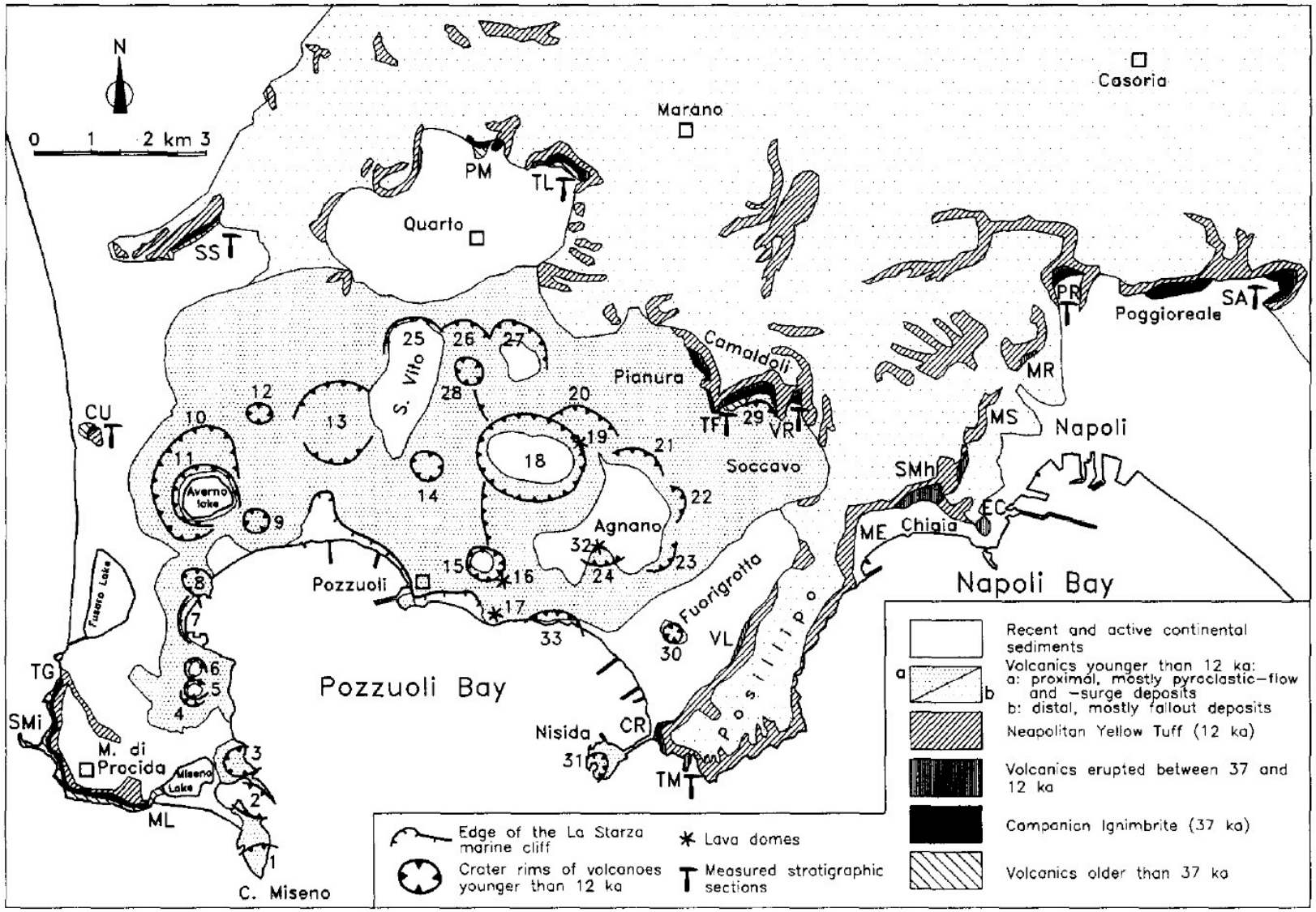

Fig. 3. Geological sketch map of the Neapolitan–Phlegraean area. *ML* = Miliscola; *SMi* = San Martino islet; *TG* = Torregaveta; *CU* = Cuma; *SS* = San Severino; *PM* = Punta Marmolite; *TL* = Trefola; *TF* = Torre di Franco; *VR* = Verdolino; *PR* = Ponti Rossi; *SA* = Sant'Arpino; *MR* = Moiariello; *MS* = Montesanto; *ME* = Mergellino; *SMh* = San Martino hill; *EC* = Monte Echia; *TM* = Trentaremi; *CR* = Coroglio; *VL* = Villanova. Location of vents is indicated by numerals on the map: *1* = Capo Miseno; *2* = Punta Pennata; *3* = Bacoli; *4* = Bellavista; *5* = Fondi di Baia I; *6* = Fondi di Baia II; *7* = Baia; *8* = Mofete; *9* = Monte Nuovo; *10* = Archiaverno; *11* = Averno; *12* = Fondo Riccio; *13* = Gauro; *14* = Cigliano; *15* = Solfatara; *16* = Accademia; *17* = Monte Olibano; *18* = Astroni; *19* = Caprara; *20* = Sartania; *21* = Pigna San Nicola; *22* = Monte Sant'Angelo; *23* = Grotta del Cane; *24* = Agnano–Monte Spina; *25* = Montagna Spaccata; *26* = Pisani; *27* = San Martino; *28* = Senga; *29* = Minopoli; *30* = Santa Teresa; *31* = Nisida; *32* = Cupola di Monte Spina; *33* = La Pietra.

Orsi et al 1996

Campo Flegrei

Orsi et al 1996

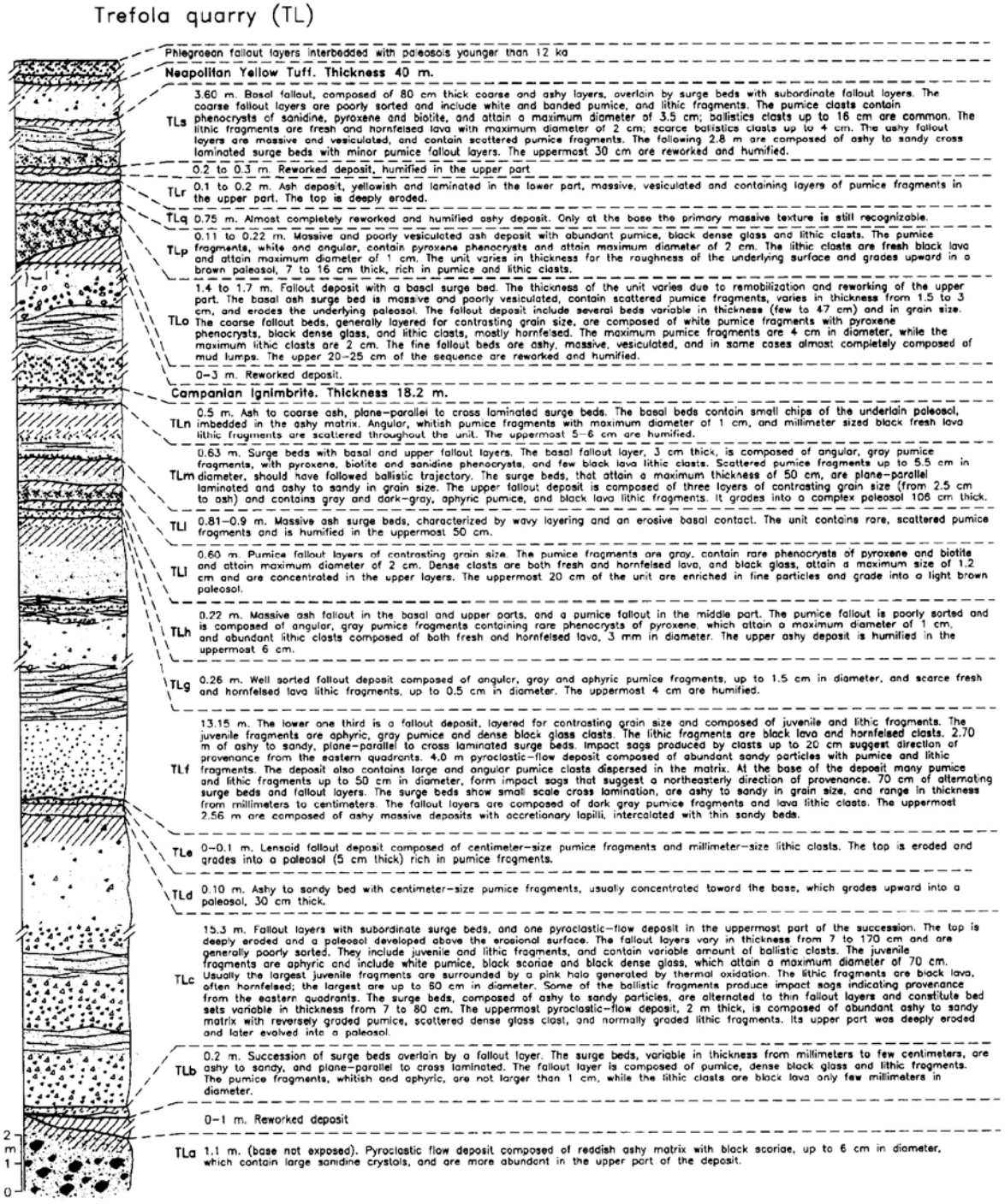

Fig. 6. Stratigraphic section measured at Trefola. For location see Fig. 3.

Campo Flegrei

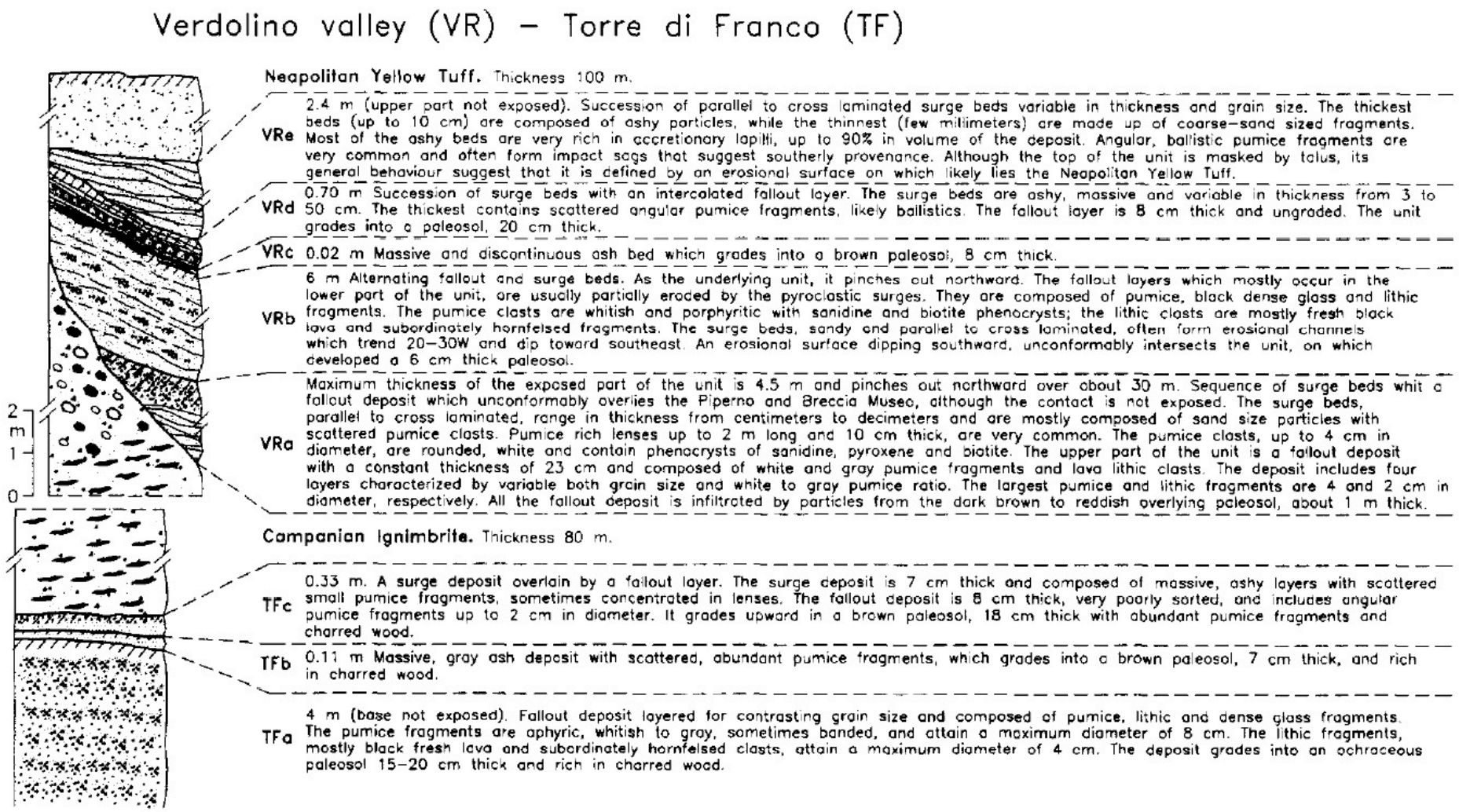

Fig. 7. Stratigraphic section measured at Verolino and Torre di Franco. For location see Fig. 3.

Orsi et al 1996

Campo Flegrei

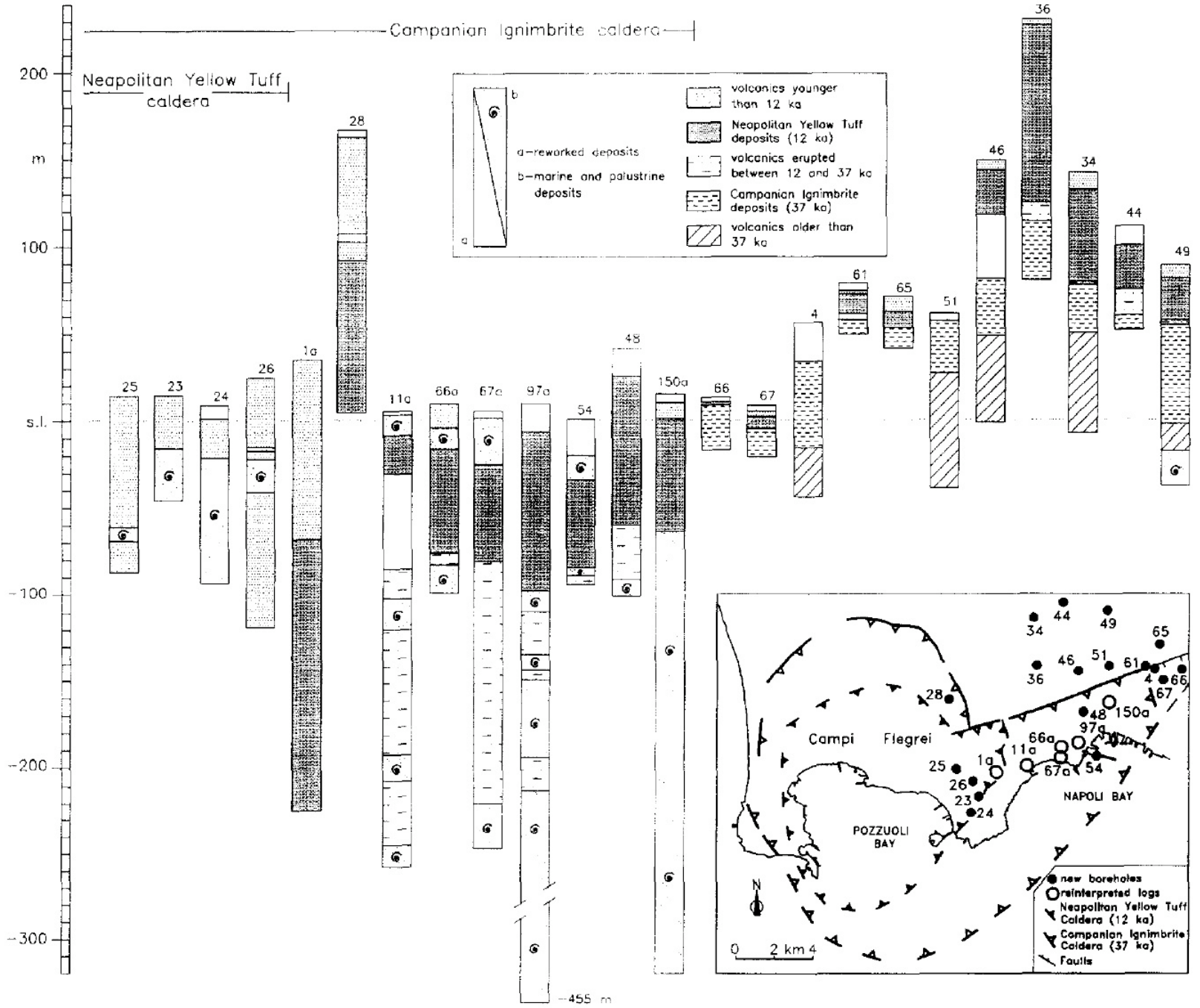

Fig. 11. Stratigraphic columns of selected boreholes.

Orsi et al 1996

Campo Flegrei

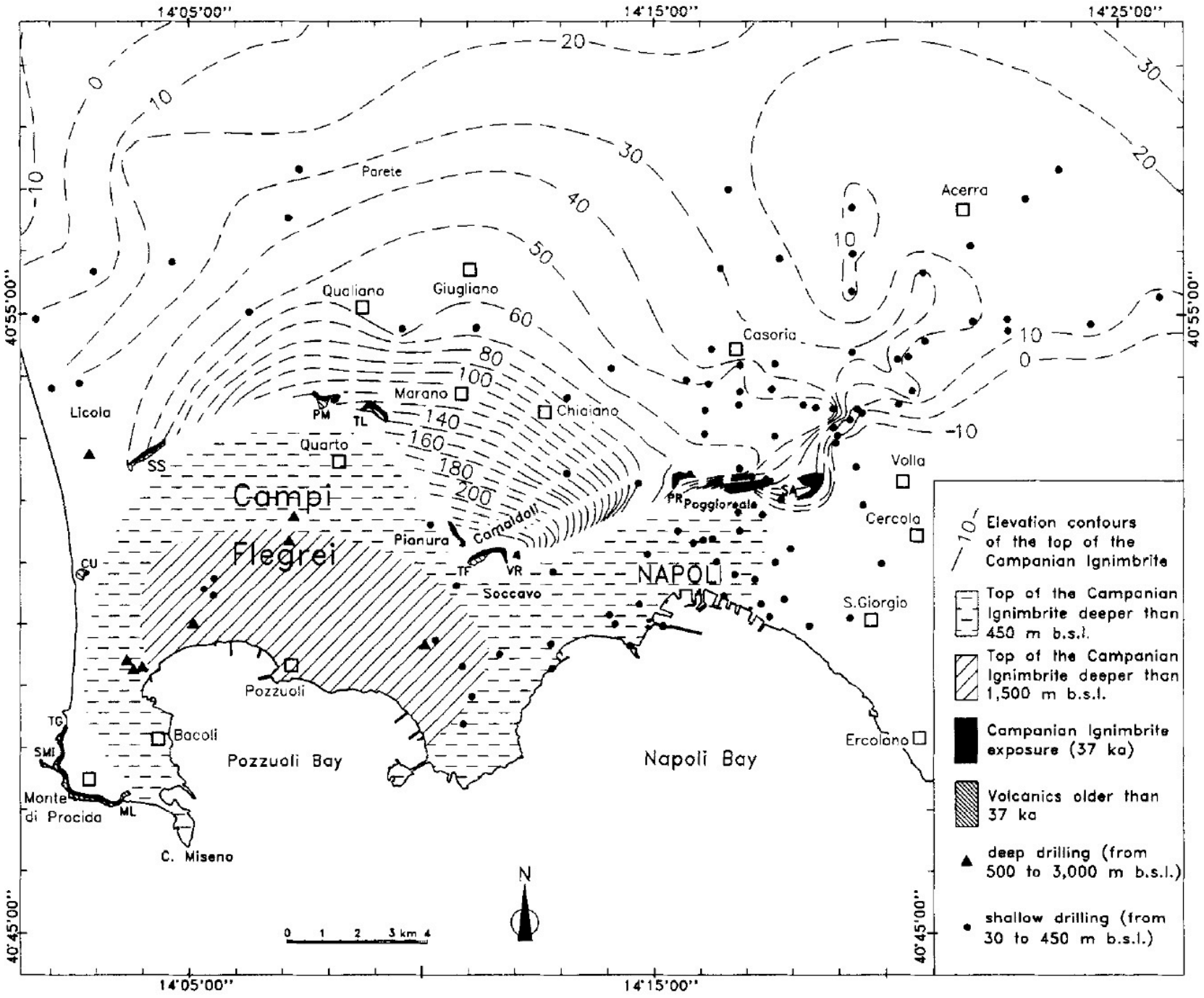

Fig. 12. Distribution of the top of the Campanian Ignimbrite.

Orsi et al 1996

Campo Flegrei

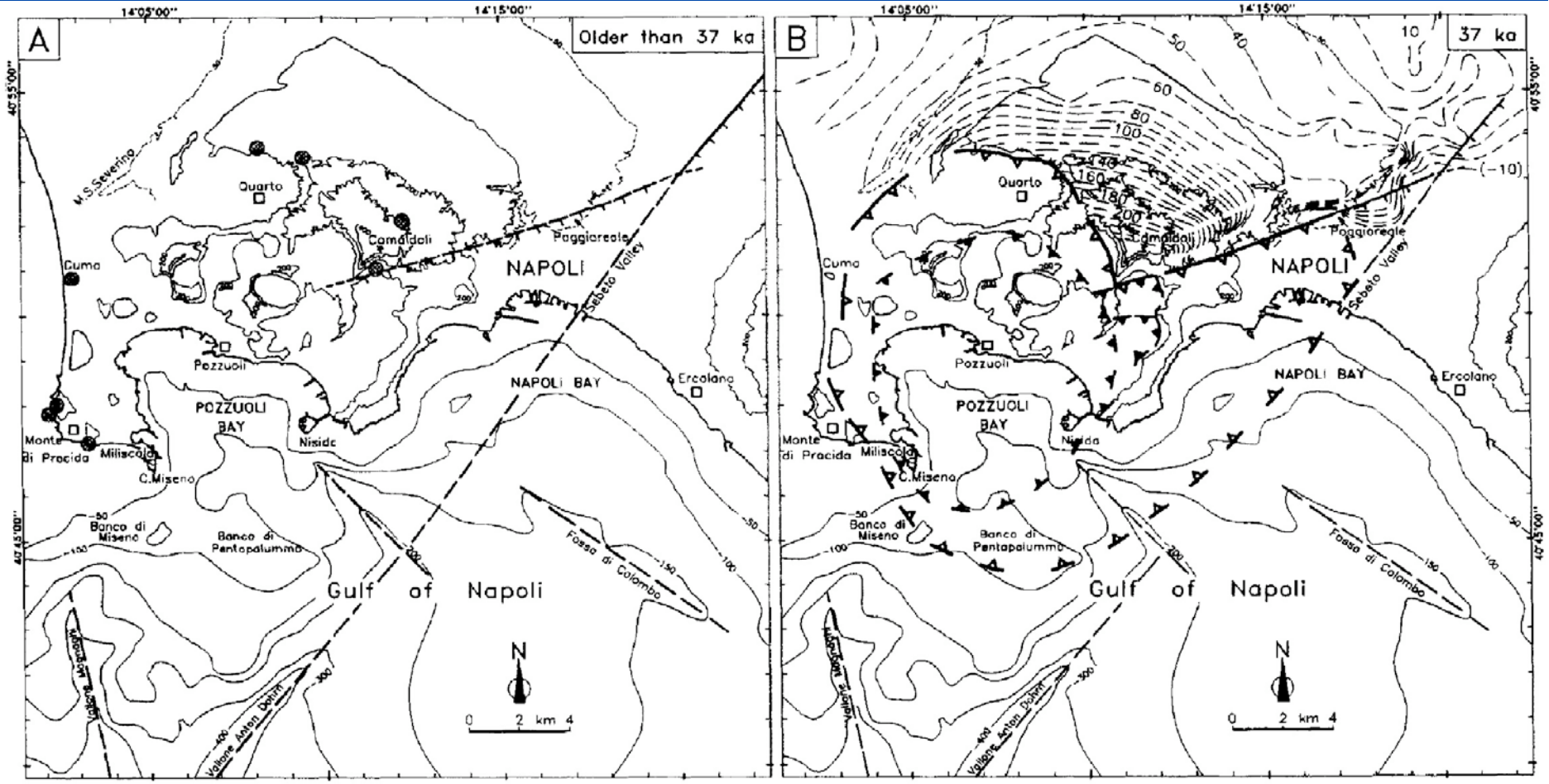

Fig. 14. Structural sketch maps of the Neapolitan–Phlegraean area showing time–space evolution of volcanism and deformations between 37 and 12 ka.

Orsi et al 1996

Campo Flegrei

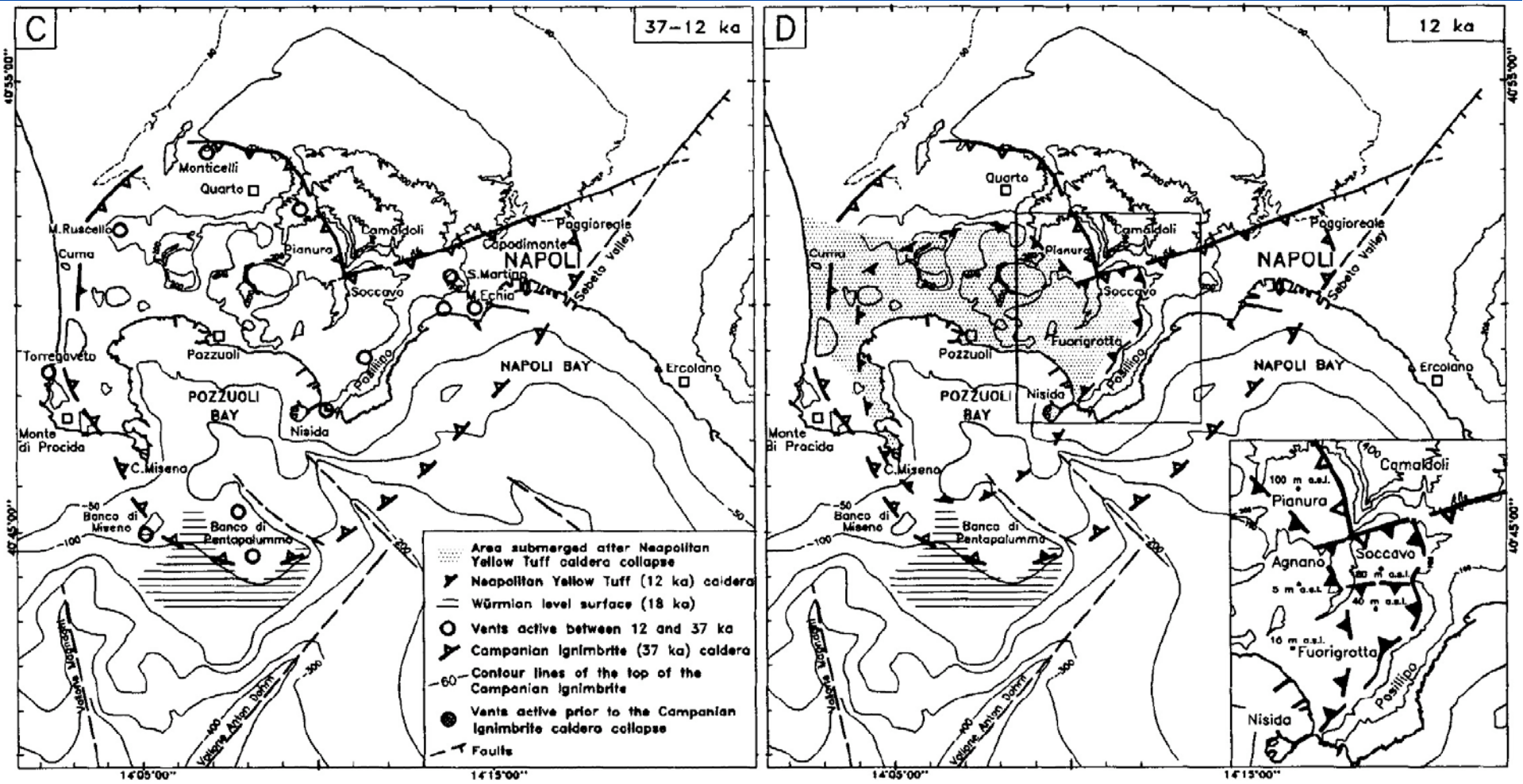

Fig. 14 (continued).

Orsi et al 1996

Campo Flegrei

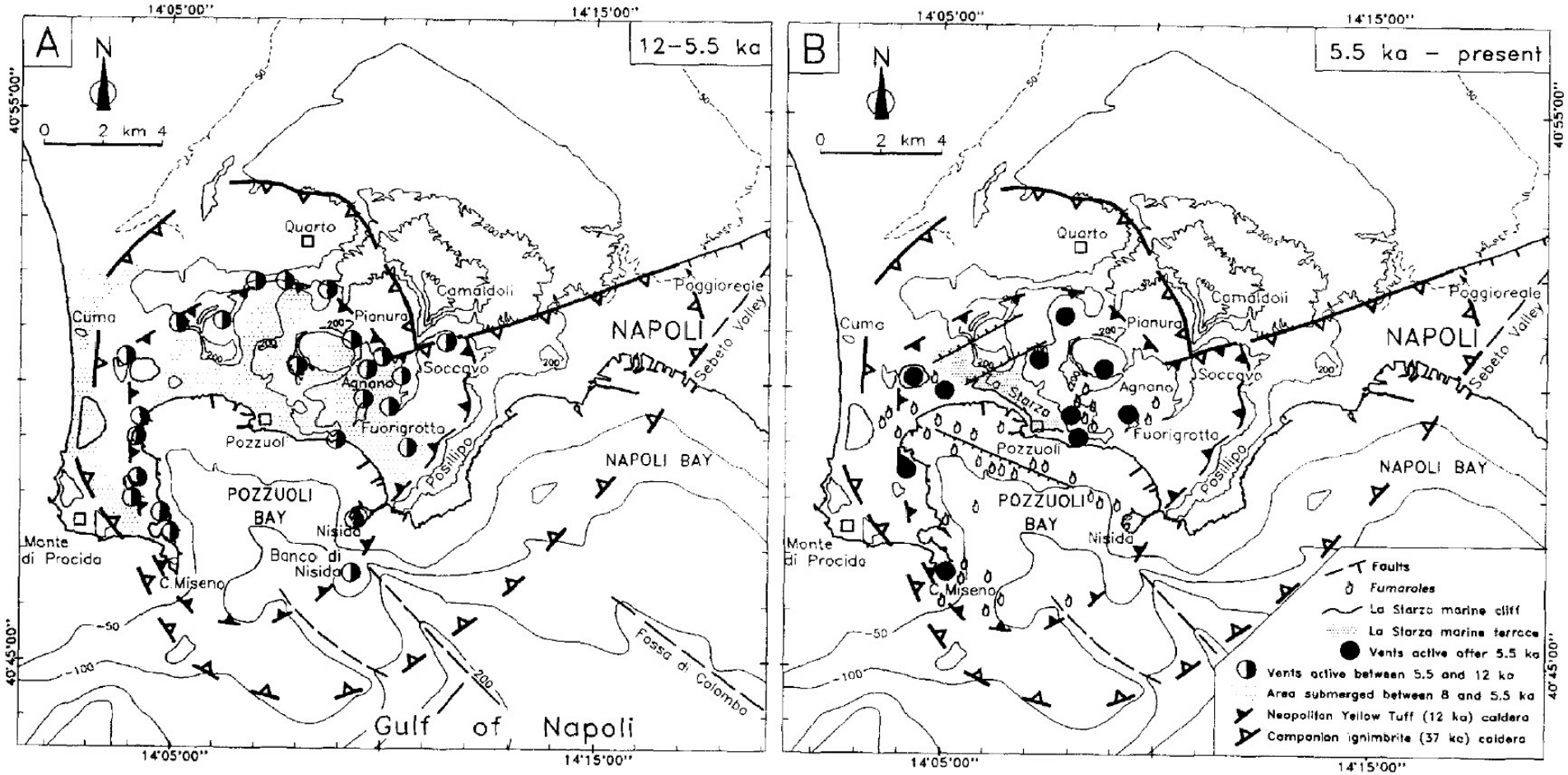

Fig. 15. Structural sketch maps of the Neapolitan–Phlegraean area showing time–space evolution of volcanism and deformations between 12 ka and present.

Orsi et al 1996

Campo Flegrei

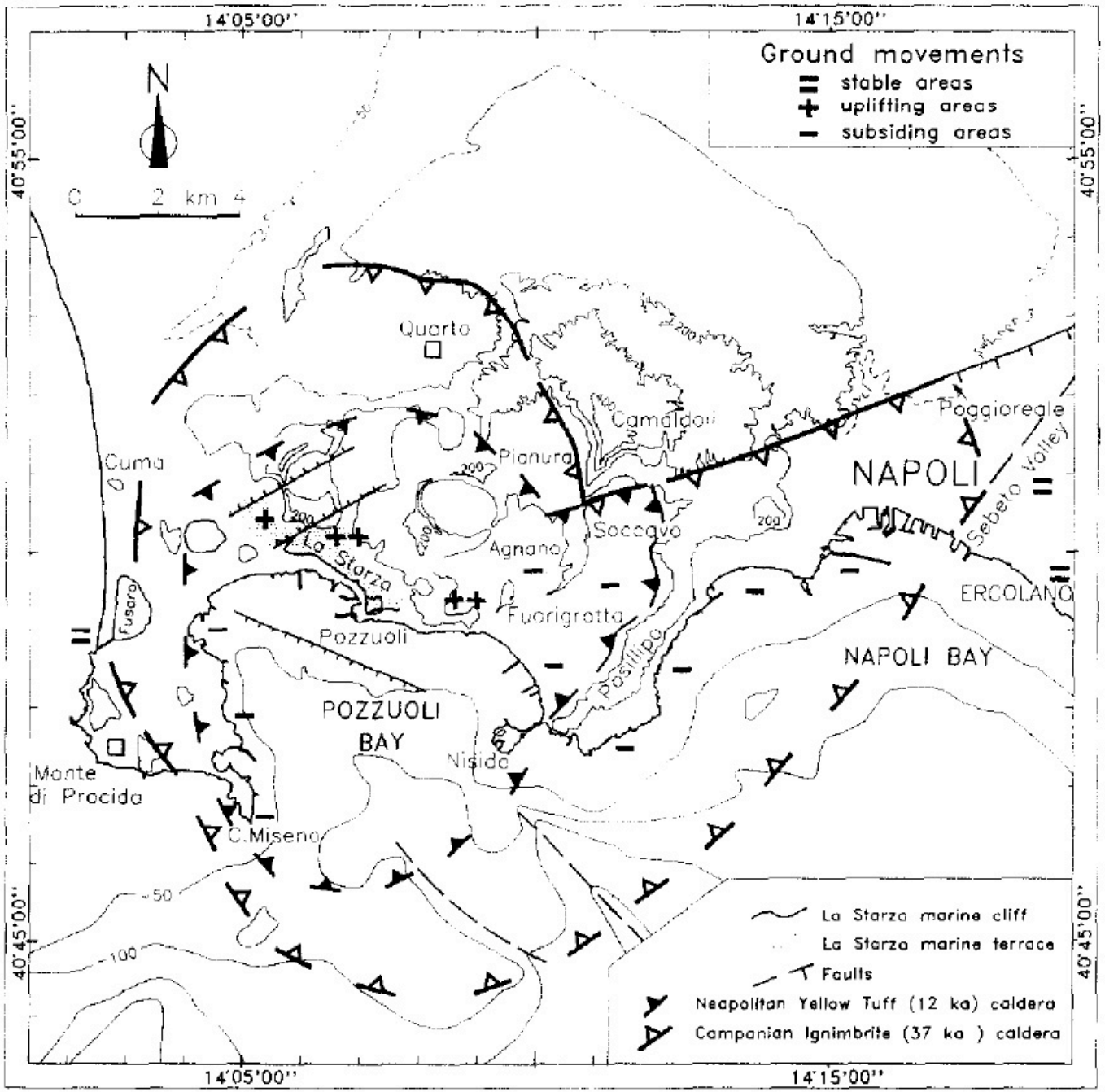

Fig. 17. Structural sketch map of the Campi Flegrei caldera.

Orsi et al 1996

Campo Flegrei

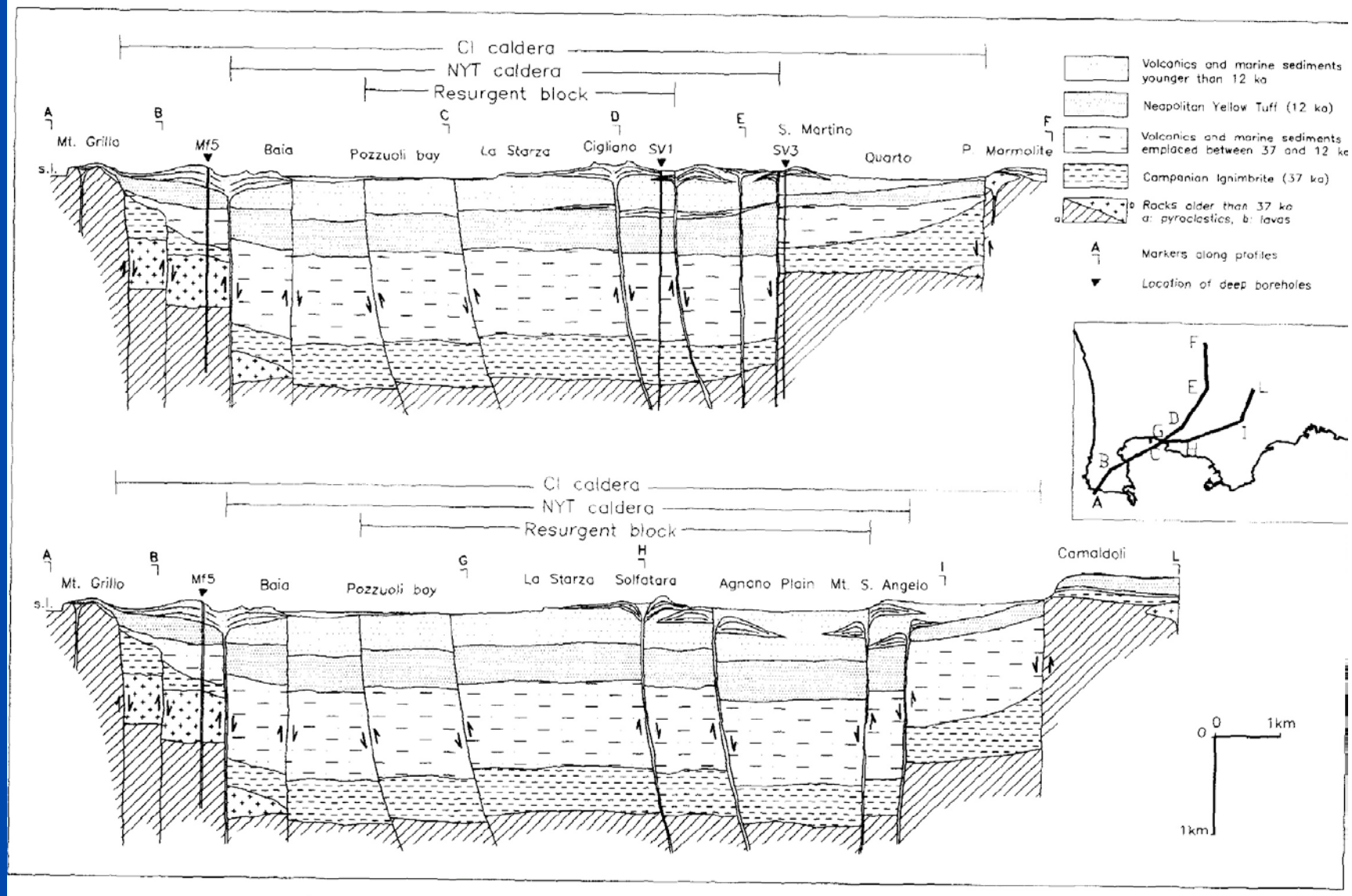

Fig. 19. Geological cross sections of the Campi Flegrei caldera; their location is reported in insert.

Orsi et al 1996